

Review

Cosmological Reflection of Particle Symmetry

Maxim Khlopov ^{1,2}

¹ Laboratory of Astroparticle Physics and Cosmology 10, rue Alice Domon et Léonie Duquet, 75205 Paris Cedex 13, France; khlopov@apc.univ-paris7.fr

² Center for Cosmoparticle Physics “Cosmion” and National Research Nuclear University “MEPHI” (Moscow State Engineering Physics Institute), Kashirskoe Shosse 31, Moscow 115409, Russia

Academic Editor: Sergei D. Odintsov

Received: 31 May 2016; Accepted: 10 August 2016; Published: 20 August 2016

Abstract: The standard model involves particle symmetry and the mechanism of its breaking. Modern cosmology is based on inflationary models with baryosynthesis and dark matter/energy, which involves physics beyond the standard model. Studies of the physical basis of modern cosmology combine direct searches for new physics at accelerators with its indirect non-accelerator probes, in which cosmological consequences of particle models play an important role. The cosmological reflection of particle symmetry and the mechanisms of its breaking are the subject of the present review.

Keywords: elementary particles; dark matter; early universe; symmetry breaking

1. Introduction

The laws of known particle interactions and transformations are based on the gauge symmetry-extension of the gauge principle of quantum electrodynamics to strong and weak interactions. Starting from isotopic invariance of nuclear forces, treating proton and neutron as different states of one particle-nucleon; the development of this approach led to the successful creation of the modern standard model of the elementary particle, involving symmetry between different particles and ascribing their difference to the mechanisms of symmetry breaking. However successful the standard model (SM) is in describing particle properties and interactions, it is not sufficient to provide the basis for modern inflationary cosmology with baryosynthesis and dark matter/energy, and it should be extended to resolve its internal problems, such as divergence of mass of the Higgs boson (which may be resolved by supersymmetric extensions of the SM) or CP violation in Quantum Chromodynamics (QCD) (a popular solution which involves additional Peccei–Quinn symmetry). The aesthetic argument for the extension of the SM comes from the possibility to unify strong and electroweak interactions in the framework of Grand Unified Theories (GUT). The discovery of nonzero mass of neutrino—reflected in the experimentally-detected neutrino oscillations—has already moved physics beyond the SM, since in the SM, neutrinos are massless.

Extensions of the standard model involve new symmetries and new particle states. Noether’s theorem relates the exact particle symmetry to conservation of respective charge. If the symmetry is strict, the charge is strictly conserved. The lightest particle bearing this charge is stable. Born in the Universe, they should be present in the form of dark matter, corresponding to $\sim 25\%$ of the total cosmological density. This form of matter (see, e.g., References [1–6] for review and reference) should be stable, explain the measured dark matter density, and decouple from plasma and radiation at least before the beginning of the matter dominated stage. Formation of the large scale structure of the universe from small initial density fluctuations is one of the most important reasons for the *nonbaryonic* nature of the dark matter that is decoupled from matter and radiation, and provides the effective growth of these fluctuations before recombination. It implies dark matter candidates from the physics beyond the standard model (see References [6–10] for recent review).

On the other hand, the initial density fluctuations coming from the very early universe are also originated from physics beyond the standard model. Mechanisms of symmetry breaking induce new fundamental physical scales in particle theory. If the symmetry is spontaneously broken, it is restored when the temperature exceeds the corresponding scale. Such high temperatures should have naturally arisen at the early stages of cosmological evolution. In the course of cosmological expansion, the temperature decreased, and the transition to the phase with broken symmetry took place, which may be reflected in observable cosmological consequences.

It makes the Big Bang Universe a natural laboratory of particle physics, not only due to possibility of the creation of hypothetical stable particles in the early universe, but also owing to the reflection of the hierarchy of particle symmetry breaking in cosmological phase transitions in their observable effects.

In the old Big Bang scenario, cosmological expansion and its initial conditions were given a priori [11,12]. In modern cosmology, expansion of the universe and its initial conditions are related to inflation [13–17], baryosynthesis [18,19], and nonbaryonic dark matter (see review in References [20–23]). The global properties of the universe, as well as the origin of its large scale structure are considered as the result of the process of inflation. The matter content of the modern universe is also originated from the physical processes: the baryon density is the result of baryosynthesis, and the nonbaryonic dark matter represents the relic species of physics beyond the standard model.

These basic elements of modern cosmology are related with physics beyond the standard model, and in various aspects reflect particle symmetry and mechanisms of its breaking. New symmetries are implied to protect the stability of dark matter candidates. CP violation and baryon charge nonconservation are needed for the generation of baryon excess in a baryon symmetric universe. New fields are needed to drive inflation and play the role of the inflaton. Such fields were associated in the old inflationary scenario [14] with the Higgs mechanism of symmetry breaking in Grand Unified Theories (GUT). Inflation finds a relationship with supergravity models in some recent approaches [24].

Whatever the extension of the Standard Model which describes these necessary basic elements of modern cosmology, such extensions inevitably contain some additional model-dependent cosmological consequences, and here we would like to discuss [25] various forms of such additional cosmological reflections of the fundamental particle symmetry. The presented list of nontrivial examples of such reflections—being far from complete—is challenging for the development of astrophysical, astroparticle, cosmological, and collider probes for new physics.

In Section 2 we present examples of the cosmological pattern of particle symmetry and its breaking, from various types of particle dark matter candidates to primordial nonlinear structures. We then consider primordial black holes as universal theoretical probes for cosmological consequences of particle theory (Section 3). We relate the observed broken symmetry of the three known families to various types of dark matter embedded in a unique framework of horizontal unification as well as discuss a possibility for stable charged species of new quarks and leptons to form dark matter, hidden in neutral dark atoms (Section 4). In Section 5 we consider the simplest case of heavy stable -2 charged lepton-like particles surrounded by a helium nuclear shell that form nuclear-interacting O-helium (OHe) dark atoms. The qualitative advantages of using this OHe scenario to explain several puzzles of direct and indirect searches for dark matter challenge its test at the Large Hadron Collider (LHC). The conclusive Section 6 considers cosmological probes of fundamental particle structure in the context of cosmoparticle physics, studying the fundamental relationship of micro- and macro- worlds.

2. Cosmological Pattern of Particle Physics

In the following, we will specify possible links between fundamental particle structure and its cosmological effects.

Most of the known particles are unstable. For a particle with the mass m , the particle physics time scale is $t \sim 1/m$ (Henceforth, if it is not otherwise specified, we use the units $\hbar = c = k = 1$), so in

the particle world we refer to particles with lifetime $\tau \gg 1/m$ as metastable. To be of cosmological significance in the Big Bang Universe, a metastable particle should survive after $t \sim (m_{pl}/m^2)$, when the temperature of the universe T fell below $T \sim m$, and particles go out of thermal equilibrium. It means that the particle lifetime should exceed $t \sim (m_{pl}/m) \cdot (1/m)$, and such a long lifetime should be explained by the existence of an (approximate) symmetry. From this viewpoint, cosmology is sensitive to the conservation laws reflecting strict or nearly strict symmetries of particle theory.

The stability of our ordinary (baryonic) matter gives us an example of this relationship, being protected by the conservation of electric and baryon charges. We assume that an electron is absolutely stable, owing to the conservation of electric charge, while the stability of a proton is conditioned by the conservation of baryon charge. According to the SM, the properties of ordinary matter reflect the fundamental physical scales of electroweak and strong interactions. The mass of an electron is originated from the Higgs mechanism of electroweak symmetry breaking, whereas the mass of a proton reflects the scale of QCD confinement.

New stable particles, corresponding to the new strict symmetry, should be present in the universe and play the role of cosmological dark matter.

However, there is no strict symmetry between various quarks and leptons. Symmetry breaking implies the difference in particle masses. The particle mass spectrum reflects the hierarchy and structure of symmetry breaking.

The mechanism of the spontaneous breaking of particle symmetry also has a cosmological impact. Heating of the condensed matter leads to the restoration of its symmetry. When the heated matter cools down, phase transition to the phase of broken symmetry takes place. In the course of the phase transitions—corresponding to the given type of symmetry breaking—topological defects can form. One can directly observe the formation of such defects in liquid crystals or in superfluid He. In the same manner, the mechanism of the spontaneous breaking of particle symmetry implies the restoration of the underlying symmetry in the early universe at high temperatures.

When temperature decreases in the course of cosmological expansion, transitions to the phase of broken symmetry can lead—depending on the symmetry breaking pattern—to the formation of topological defects in the very early universe. Defects can represent new forms of stable particles (as in the case of magnetic monopoles [26–31]), or extended macroscopic structures, such as cosmic strings [32,33] or cosmic walls [34].

2.1. Cosmoarcheology of New Physics

Cosmoarcheology considers the results of observational cosmology as the sample of the experimental data on the possible existence and features of hypothetical forms of matter predicted by particle theory. It undertakes a *Gedanken Experiment* with these forms, assuming some theoretical framework for the origin and evolution of the universe [4].

One can specify new forms of matter by their net contribution to cosmological density and by their possible influence on parameters of matter and radiation.

If new forms of matter lend a dominant contribution to the density of the universe, they determine the dynamics of expansion in that period. The contribution of subdominant new forms of matter to the total density is always small. The simplest examples are dominant and subdominant forms of dark matter.

The effects of new forms of matter can be time dependent, being characterized by their time-scale. Particle decays, evaporation of primordial black holes or the development of gravitational instability are examples of such time dependent effects.

The cosmological structures predicted by particle theory can have inhomogeneous distribution in space. The amplitude of density fluctuations $\delta \equiv \delta q/q$ measures the level of inhomogeneity relative to the total density, q . The partial amplitude $\delta_i \equiv \delta q_i/q_i$ measures the level of fluctuations within a particular component with density q_i contributing to the total density $q = \sum_i q_i$. The case $\delta_i \geq 1$ within the considered i -th component corresponds to its strong inhomogeneity. Strong inhomogeneity

is compatible with the smallness of total density fluctuations if the contribution of the inhomogeneous component into the total density is small: $q_i \ll q$, so that $\delta \ll 1$ (see Reference [35] for review).

The presence of new forms of matter can influence the properties of matter and radiation either indirectly (i.e., changing the cosmological equation of state) or via direct interaction with matter and radiation. In the first case, only the dominant forms of matter are relevant. In the second case, effects of even subdominant forms of matter are accessible to observational data. The detailed analysis of the sensitivity of cosmological data to various phenomena of new physics are presented in References [1,25].

It should be noted that the parameters of physics beyond the SM can relate the accessible effects to direct experimental research at the accelerators to the cosmological effects of new physics. So, in the model of horizontal unification [36–39], the top quark (or B-meson) physics fixes the parameters, describing the dark matter, while in supersymmetric models, experimental searches for unstable SUSY (supersymmetric) particles at the LHC put constraints on the parameters of SUSY dark matter candidates [40].

2.2. Cosmophenomenology of New Stable Particles

To study the imprints of new physics in astrophysical data, cosmoarcheology implies the forms and means in which new physics leaves such imprints. So, the important tool of cosmoarcheology in linking the cosmological predictions of particle theory to observational data is the *Cosmophenomenology* of new physics. It studies the possible hypothetical forms of new physics (which may appear as cosmological consequences of particle theory) and their properties, which can result in observable effects.

2.2.1. Freezing out

The simplest primordial form of new physics is the gas of new stable massive particles, originated from the early universe. For particles with mass m , at high temperature $T > m$, their number density is $n \sim T^3$, and the equilibrium condition

$$n \cdot \sigma v \cdot t > 1 \quad (1)$$

is valid at $t \sim mPl/T^2$ if their annihilation cross section $\sigma > 1/(TmPl)$ is sufficiently large to support the equilibrium. At $T < m$, such particles go out of equilibrium and their relative concentration freezes out. This is the main idea of the calculation of primordial abundance for Weakly Interacting Massive Particles (WIMPs, see References [1,4] for details).

If ordinary particles are among the products of WIMP annihilation, even their small fraction can annihilate in the galaxy, causing significant effects in cosmic rays and gamma background. This effect—first revealed in Reference [41] and then proven for even subdominant fraction of annihilating dark matter in Reference [42]—is now the basis of indirect dark matter searches in cosmic rays [40].

The process of WIMP annihilation to ordinary particles, considered in t channel, determines their scattering cross section on ordinary particles, and thus relates the primordial abundance of WIMPs to their scattering rate in ordinary matter. Forming a nonluminous massive halo of our galaxy, WIMPs can penetrate terrestrial matter and scatter on nuclei in underground detectors. The strategy of direct WIMP searches implies the detection of recoil nuclei from this scattering.

The process inverse to the annihilation of WIMPs corresponds to their production in the collisions of ordinary particles. It should lead to effects of missing mass and energy-momentum, being the challenge of the experimental search for the production of dark matter candidates at accelerators—e.g., at the LHC.

2.2.2. Stable Relics: Decoupling

More weakly interacting and/or more light species decouple from plasma and radiation, being relativistic at $T \gg m$, when

$$n \cdot \sigma v \cdot t \sim 1 \quad (2)$$

i.e., at

$$T_{dec} \sim (\sigma m_{Pl})^{-1} \gg m \quad (3)$$

After decoupling, these species retain their equilibrium distribution until they become non-relativistic at $T < m$. Conservation of partial entropy in the cosmological expansion links the modern abundance of these species to the number density of relic photons with the account for the increase of the photon number density due to the contribution of heavier ordinary particles, which were in equilibrium in the period of decoupling.

For example, primordial neutrino decouple in the period when relativistic electron-positron plasma was present in equilibrium. The account for the increase of the number density of relic photons due to electron-positron annihilation at $T < m_e$ —where m_e is the mass of an electron—results in the well-known prediction of Big Bang cosmology [11,12]

$$n_{\nu\bar{\nu}} = \frac{3}{11} n_\gamma \quad (4)$$

where $n_{\nu\bar{\nu}}$ is the modern number density of one species of primordial left-handed neutrinos (and the corresponding antineutrinos) and $n_\gamma = 400 \text{ cm}^{-3}$ is the number density of Cosmological Microwave Background (CMB) photons at the modern CMB temperature $T = 2.7 \text{ K}$. Multiplying the predicted modern concentration of neutrinos by their mass, we obtain their contribution to the total density. This contribution should not exceed the total density, which gave the early cosmological upper limits on neutrino mass. For a long time, it seemed possible that relic neutrinos could be the dominant form of cosmological dark matter, and the corresponding neutrino-dominated universe was considered as the physical ground of the Hot Dark Matter scenario of large scale structure formation. Experimental discovery of neutrino oscillations, together with stringent upper limits on the mass of an electron neutrino, exclude this possibility. Moreover, even neutrino masses in the range of 1 eV lead to features in the spectrum of density fluctuations that are excluded by the observational data of CMB.

Right-handed neutrinos and left-handed antineutrinos, involved in the seesaw mechanism of neutrino mass generation, are sterile relative to ordinary weak interaction. If these species were in thermal equilibrium in the early universe, they should decouple much earlier than ordinary neutrinos in the period when there were much more particle species (leptons, quarks, gluons, etc.) in the equilibrium, what leads to the primordial abundance of sterile neutrinos much smaller than the ordinary ones. Therefore, cosmological constraints permit sterile neutrinos with mass in the keV range. We refer to the Reference [43] for a recent review of models of sterile neutrinos and their possible effects.

2.2.3. Stable Relics: SuperWIMPs

The maximal temperature which is reached in inflationary universe is the reheating temperature, T_r , after inflation. So, the very weakly interacting particles with the annihilation cross section

$$\sigma < 1/(T_r m_{Pl}) \quad (5)$$

as well as very heavy particles with mass

$$m \gg T_r \quad (6)$$

cannot be in thermal equilibrium, and the detailed mechanism of their production should be considered to calculate their primordial abundance.

In particular, the thermal production of the gravitino in the very early universe is proportional to the reheating temperature T_r , which puts an upper limit on this temperature from constraints on primordial gravitino abundance [44–50].

2.2.4. Self-Interacting Dark Matter

Extensive hidden sector of particle theory can provide the existence of new interactions, which only new particles possess. Historically, one of the first examples of such self-interacting dark matter was presented by the model of mirror matter. Mirror particles—first proposed by T. D. Lee and C. N. Yang [51] to restore the equivalence of left- and right-handed co-ordinate systems in the presence of P- and C-violation in weak interactions—should be strictly symmetric by their properties to their ordinary twins. After the discovery of CP-violation, it was shown by I. Yu. Kobzarev, et al. in Reference [52] that mirror partners cannot be associated with antiparticles and should represent a new set of symmetric partners for ordinary quarks and leptons with their own strong, electromagnetic, and weak mirror interactions. It means that there should exist mirror quarks, bound in mirror nucleons by mirror QCD forces and mirror atoms, in which mirror nuclei are bound with mirror electrons by mirror electromagnetic interaction [53,54]. If gravity is the only common interaction for ordinary and mirror particles, mirror matter can be present in the universe in the form of elusive mirror objects, having symmetric properties with ordinary astronomical objects (gas, plasma, stars, planets, etc.), but causing only gravitational effects on ordinary matter [55,56].

Even in the absence of any other common interaction except for gravity, the observational data on primordial helium abundance and the upper limits on local dark matter seem to exclude mirror matter evolving in the universe in a fully symmetric way in parallel with the ordinary baryonic matter [57,58]. The symmetry in the cosmological evolution of mirror matter can be broken either by initial conditions [59,60] or by breaking mirror symmetry in the sets of particles and their interactions as it takes place in the shadow world [61,62], arising in the heterotic string model. We refer to References [2,63,64] for a current review of mirror matter and its cosmology.

If new particles possess new y -charge, interacting with massless bosons or intermediate bosons with sufficiently small mass (y -interaction), for slow y -charged particles a Coulomb-like factor of “Gamov–Sommerfeld–Sakharov enhancement” [65–67] should be added in the annihilation cross section

$$C_y = \frac{2\pi\alpha_y/v}{1 - \exp(-2\pi\alpha_y/v)} \quad (7)$$

where v is relative velocity and α_y is the running gauge constant of the y -interaction. This factor may not be essential in the period of particle freezing out in the early universe (when v was only a few times smaller than c), but can cause strong enhancement in the effect of annihilation of nonrelativistic dark matter particles in the galaxy.

2.2.5. Subdominant Dark Matter

If charge-symmetric stable particles (and their antiparticles) represent the only subdominant fraction of cosmological dark matter, a more detailed analysis of their distribution in space, of their condensation in galaxies, of their capture by stars, Sun, and Earth, as well as the effects of their interaction with matter and of their annihilation provides more sensitive probes for their existence.

In particular, fourth-generation hypothetical stable neutrinos with mass about 50 GeV should be the subdominant form of modern dark matter, contributing less than 0.1% to the total density [41,42]. However, direct experimental search for cosmic fluxes of weakly interacting massive particles (WIMPs) may be sensitive to existence of such components (see [68–76] and references therein). It was shown in References [77–80] that annihilation of fourth generation neutrinos and their antineutrinos in the galaxy is severely constrained by the measurements of gamma-background, cosmic positrons, and antiprotons. Fourth generation neutrino annihilation inside the Earth should lead to the flux of

underground monochromatic neutrinos of known types, which can be traced in the analysis of the already existing and future data of underground neutrino detectors [79,81–83].

2.2.6. Charged Stable Relics: Dark Atoms

New particles with electric charge and/or strong interaction can form anomalous atoms and be contained in ordinary matter as anomalous isotopes. For example, if the lightest fourth generation quark is stable, it can form stable charged hadrons, serving as nuclei of anomalous atoms of, for example, anomalous helium [84–89]. Therefore, stringent upper limits on anomalous isotopes, especially on anomalous hydrogen, put severe constraints on the existence of new stable charged particles. However, as we discuss in Section 4, stable doubly charged particles cannot only exist, but even dominate in cosmological dark matter, being effectively hidden in neutral “dark atoms” [90].

2.3. Cosmophenomenology of Metastable Particles

2.3.1. Decaying Dark Matter

Decaying particles with lifetime τ , exceeding the age of the universe (t_U , $\tau > t_U$) can be treated as stable. By definition, primordial stable particles survive to the present time and should be present in the modern universe. The net effect of their existence is given by their contribution to the total cosmological density. However, even the small effect of their decay can lead to a significant contribution to cosmic rays and gamma background [91]. Leptonic decays of dark matter are considered as a possible explanation of the cosmic positron excess, measured in the range above 10 GeV by PAMELA [92], FERMI/LAT [93], and AMS02 [94] (see Reference [95] for a review of the AMS02 experiment).

2.3.2. Charge Asymmetry of Dark Matter

The fact that particles are not absolutely stable means that the corresponding charge is not strictly conserved and the generation of particle charge asymmetry is possible, as is assumed for ordinary baryonic matter. At sufficiently strong particle annihilation cross section, excessive particles (antiparticles) can dominate in the relic density, leaving an exponentially small admixture of their antiparticles (particles) in the same way that primordial excessive baryons dominate over antibaryons in the baryon asymmetric universe. In this case, *asymmetric dark matter* does not lead to a significant effect of particle annihilation in the modern universe and can be searched for either directly in underground detectors or indirectly by effects of decay or condensation and structural transformations of, e.g., neutron stars (see Reference [96] for recent review and references). If particle annihilation is not strong enough, primordial pairs of particles and antiparticles dominate over excessive particles (or antiparticles), and this case has no principle difference from the charge symmetric case. In particular, for very heavy charged leptons (with mass above 1 TeV), like “tera electrons” [97], discussed in Section 4.2, their annihilation due to electromagnetic interaction is too weak to provide effective suppression of primordial tera electron–positron pairs relative to primordial asymmetric excess [84].

2.3.3. Unstable Particles

Primordial unstable particles with a lifetime less than the age of the universe ($\tau < t_U$) cannot survive to the present time. However, if their lifetime is sufficiently large to satisfy the condition $\tau \gg (m_{Pl}/m) \cdot (1/m)$, their existence in the early universe can lead to direct or indirect traces [98].

Weakly interacting particles decaying to invisible modes can influence large scale structure formation. Such decays prevent the formation of structure if they take place before the structure is formed. Invisible products of decays after the structure is formed should contribute to the cosmological dark energy. The unstable dark matter [39,99–106] implied weakly interacting particles that form structure in the matter-dominated stage and then decay to invisible modes after the structure is formed.

The cosmological flux of decay products contributing to the cosmic and gamma ray backgrounds represents the direct trace of unstable particles [98,107]. If the decay products do not survive to the

present time, their interaction with matter and radiation can cause indirect trace in the light element abundance [46–48,108] or in the fluctuations of thermal radiation [109].

If the particle lifetime is much less than 1 s, the multi-step indirect traces are possible, provided that particles dominate in the universe before their decay. In the dust-like stage of their dominance, black hole formation takes place, and the spectrum of such primordial black holes traces the particle properties (mass, frozen concentration, lifetime) [110–112]. The particle decay in the end of the dust-like stage influences the baryon asymmetry of the universe. Cosmophenomenological chains link the predicted properties of even unstable new particles to the effects accessible in astronomical observations. Such effects may be important in the analysis of the observational data.

2.4. Phase Transitions

Parameters of new stable and metastable particles are also determined by a pattern of particle symmetry breaking. This pattern is reflected in a succession of phase transitions in the early universe. First order phase transitions proceed through bubble nucleation, which can result in black hole formation (see References [113,114] for review and references). Phase transitions of the second order can lead to the formation of topological defects, such as walls, string, or monopoles. The observational data puts severe constraints on magnetic monopole [28] and cosmic wall production [34], as well as on the parameters of cosmic strings [32,33]. The structure of cosmological defects can be changed in a succession of phase transitions. More complicated forms, like walls-surrounded-by-strings, can appear. Such structures can be unstable, but their existence can leave a trace in the nonhomogeneous distribution of dark matter and give rise to large scale structures of nonhomogeneous dark matter like *archioles* [115–117]. This effect should be taken into account in the analysis of the cosmological effects of weakly interacting slim particles (WISPs) (see Reference [118] for current review) that can play the role of cold dark matter in spite of their small mass.

A wide class of particle models possesses a symmetry breaking pattern, which can be effectively described by pseudo-Nambu–Goldstone (PNG) field and which corresponds to the formation of unstable topological defect structure in the early universe (see Reference [114] for review and references). The Nambu–Goldstone nature in such an effective description reflects the spontaneous breaking of global U(1) symmetry, resulting in continuous degeneracy of vacua. The explicit symmetry breaking at smaller energy scale changes this continuous degeneracy by discrete vacuum degeneracy. The character of formed structures is different for phase transitions, taking place on post-inflationary and inflationary stages.

2.4.1. Large Scale Correlations of Axion Field

At high temperatures, such a symmetry breaking pattern implies the succession of second order phase transitions. In the first transition, continuous degeneracy of vacua leads—at scales exceeding the correlation length—to the formation of topological defects in the form of a string network; in the second phase transition, continuous transitions in space between degenerated vacua form surfaces: domain walls surrounded by strings. This last structure is unstable, but, as was shown in the example of the invisible axion [115–117], it is reflected in the large scale inhomogeneity of the distribution of the energy density of coherent PNG (axion) field oscillations. This energy density is proportional to the initial phase value, which acquires a dynamical meaning of the amplitude of the axion field, when axion mass is switched on as a result of the second phase transition.

The value of phase changes by 2π around string. This strong nonhomogeneity of phase leads to corresponding nonhomogeneity of the energy density of coherent PNG (axion) field oscillations. The usual argument (see Reference [119] and references therein) is essential only at scales corresponding to the mean distance between strings. This distance is small, being on the order of the scale of the cosmological horizon in the period when PNG field oscillations start. However, since the nonhomogeneity of phase follows the pattern of the axion string network, this argument misses large scale correlations in the distribution of oscillations' energy density.

Indeed, numerical analysis of the string network (see the review in [120]) indicates that large string loops are strongly suppressed, and the fraction of about 80% of string length (corresponding to long loops) remains virtually the same in all large scales. This property is the other side of the well known scale invariant character of the string network. Therefore, the correlations of energy density should persist on large scales, as was revealed in References [115–117].

The large scale correlations in topological defects and their imprints in primordial inhomogeneities is the indirect effect of inflation, if phase transitions take place after the reheating of the universe. Inflation provides, in this case, the equal conditions of phase transition, taking place in causally disconnected regions.

2.4.2. Primordial Seeds for Active Galactic Nuclei

If the phase transitions take place at the inflationary stage, new forms of primordial large scale correlations appear. The example of global U(1) symmetry—broken spontaneously in the period of inflation and successively broken explicitly after reheating—was considered in Reference [121]. In this model, spontaneous U(1) symmetry breaking at the inflationary stage is induced by the vacuum expectation value $\langle \psi \rangle = f$ of a complex scalar field $\Psi = \psi \exp(i\theta)$, also having an explicit symmetry breaking term in its potential $V_{eb} = \Lambda^4(1 - \cos \theta)$. The latter is negligible in the period of inflation if $f \gg \Lambda$, so there appears a valley relative to values of phase in the field potential in this period. Fluctuations of the phase θ along this valley—being of the order of $\Delta\theta \sim H/(2\pi f)$ (here H is the Hubble parameter at the inflationary stage)—change in the course of inflation, its initial value within the regions of smaller size. Owing to such fluctuations, for the fixed value of θ_{60} in the period of inflation with e -folding $N = 60$ corresponding to the part of the universe within the modern cosmological horizon, strong deviations from this value appear at smaller scales, corresponding to later periods of inflation with $N < 60$. If $\theta_{60} < \pi$, the fluctuations can move the value of θ_N to $\theta_N > \pi$ in some regions of the universe. After reheating, when the universe cools down to temperature $T = \Lambda$, the phase transition to the true vacuum states, corresponding to the minima of V_{eb} , takes place. For $\theta_N < \pi$, the minimum of V_{eb} is reached at $\theta_{vac} = 0$; whereas in the regions with $\theta_N > \pi$, the true vacuum state corresponds to $\theta_{vac} = 2\pi$. For $\theta_{60} < \pi$ in the bulk of the volume within the modern cosmological horizon $\theta_{vac} = 0$. However, within this volume there appear regions with $\theta_{vac} = 2\pi$. These regions are surrounded by massive domain walls, formed at the border between the two vacua. Since regions with $\theta_{vac} = 2\pi$ are confined, the domain walls are closed. After their size equals the horizon, closed walls can collapse into black holes (BHs).

The mass range of formed BHs is constrained by fundamental parameters of the model, f and Λ . The maximal BH mass is determined by the condition that the wall does not dominate locally before it enters the cosmological horizon. Otherwise, local wall dominance leads to a superluminal $a \propto t^2$ expansion for the corresponding region, separating it from the other part of the universe. This condition corresponds to the mass [114]

$$M_{max} = \frac{m_{pl}}{f} m_{pl} \left(\frac{m_{pl}}{\Lambda} \right)^2 \quad (8)$$

The minimal mass follows from the condition that the gravitational radius of BH exceeds the width of wall, and it is equal to [114,122]

$$M_{min} = f \left(\frac{m_{pl}}{\Lambda} \right)^2 \quad (9)$$

Closed wall collapse leads to primordial GW spectrum, peaked at

$$\nu_0 = 3 \times 10^{11} (\Lambda/f) \text{ Hz} \quad (10)$$

with energy density up to

$$\Omega_{GW} \approx 10^{-4} (f/m_{pl}) \quad (11)$$

At $f \sim 10^{14}$ GeV this primordial gravitational wave background can reach $\Omega_{GW} \approx 10^{-9}$. For the physically reasonable values of

$$1 < \Lambda < 10^8 \text{ GeV} \quad (12)$$

the maximum of the spectrum corresponds to

$$3 \times 10^{-3} < \nu_0 < 3 \times 10^5 \text{ Hz} \quad (13)$$

In the range from tens to thousands of Hz, such background may be a challenge for Laser Interferometer Gravitational-Wave Observatory (LIGO) experiment. Another profound signature of the considered scenario are gravitational wave signals from merging of BHs in the primordial black hole (PBH) cluster. These effects can provide a test of the considered approach in Evolved Laser Interferometer Space Antenna (eLISA) experiment.

This mechanism can lead to the formation of primordial black holes of a whatever large mass (up to the mass of active galactic nuclei (AGNs) [123,124], see for latest review Reference [35]). Such black holes appear in the form of primordial black hole clusters, exhibiting fractal distribution in space [114,122,125]. This can shed new light on the problem of galaxy formation [114,124].

2.4.3. Antimatter in Baryon Asymmetric Universe?

Primordial strong inhomogeneities can also appear in the baryon charge distribution. The appearance of antibaryon domains in the baryon asymmetrical universe (reflecting the inhomogeneity of baryosynthesis) is the profound signature of such strong inhomogeneity [126]. In an example of a model of spontaneous baryosynthesis (see Reference [127] for review), the possibility of the existence of antimatter domains surviving to the present time in the inflationary universe with inhomogeneous baryosynthesis was revealed in.

The mechanism of spontaneous baryogenesis [127–129] implies the existence of a complex scalar field $\chi = (f/\sqrt{2}) \exp(\theta)$ carrying the baryonic charge. The $U(1)$ symmetry—which corresponds to the baryon charge—is broken spontaneously and explicitly. The explicit breakdown of $U(1)$ symmetry is caused by the phase-dependent term

$$V(\theta) = \Lambda^4(1 - \cos \theta) \quad (14)$$

The possible baryon and lepton number violating interaction of the field χ with matter fields can have the following structure [127]:

$$\mathcal{L} = g\chi\bar{Q}L + \text{h.c.} \quad (15)$$

where fields Q and L represent a heavy quark and lepton, coupled to the ordinary matter fields.

In the early universe, at a time when the friction term induced by the Hubble constant becomes comparable with the angular mass $m_\theta = \frac{\Lambda^2}{f}$, the phase θ starts to oscillate around the minima of the PNG potential and decays into matter fields, according to (15). The coupling (15) gives rise to the following [127]: as the phase starts to roll down in the clockwise direction (Figure 1), it preferentially creates an excess of baryons over antibaryons, while the opposite is true as it starts to roll down in the opposite direction.

The fate of such antimatter regions depends on their size. If the physical size of some of them is larger than the critical surviving size $L_c = 8h^2 \text{ kpc}$ [130], they survive annihilation with surrounding matter. The evolution of sufficiently dense antimatter domains can lead to the formation of antimatter globular clusters [131]. The existence of such clusters in the halo of our galaxy should lead to the pollution of the galactic halo by antiprotons. Their annihilation can reproduce [132] the observed galactic gamma background in the range of tens–hundreds MeV. The prediction of an antihelium component of cosmic rays [133]—accessible to future searches for cosmic ray antinuclei in PAMELA and AMS II experiments—as well as of antimatter meteorites [134] provides the direct experimental

test for this hypothesis. The possibility of the formation of dense antistars within an extension of the Affleck–Dine scenario of baryogenesis and the strategies for their search were considered in [135].

So, the primordial strong inhomogeneities in the distribution of total dark matter and baryon density in the universe is the new important phenomenon of cosmological models, based on particle models with a hierarchy of symmetry breaking.

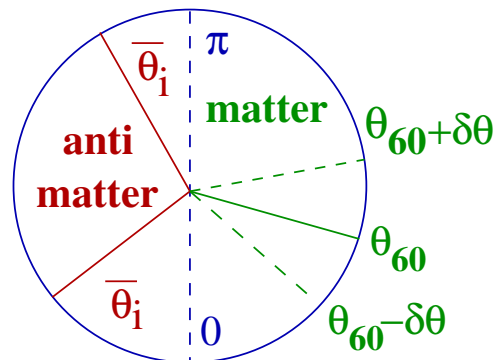


Figure 1. The inflationary evolution of the phase (taken from Reference [136]). The phase θ_{60} sits in the range $[\pi, 0]$ at the beginning of inflation and makes Brownian step $\delta\theta_{eff} = H_{infl}/(2\pi f_{eff})$ at each e-fold. The typical wavelength of the fluctuation $\delta\theta$ is equal to H_{infl}^{-1} . The whole domain H_{infl}^{-1} containing phase θ_N gets divided (after one e-fold) into e^3 causally disconnected domains of radius H_{infl}^{-1} . Each new domain contains almost homogeneous phase value $\theta_{N-1} = \theta_N \pm \delta\theta_{eff}$. This process repeats in every domain with every successive e-fold.

3. Primordial Black Holes as a Cosmological Reflection of Particle Structure

Any object of mass M can become a black hole, being put within its gravitational radius $r_g = 2GM/c^2$. At present time, black holes can be created only by a gravitational collapse of compact objects with mass more than about three solar mass [137,138]. It can be a natural end of massive stars or can result from the evolution of dense stellar clusters. However, in the early universe, there were no limits on the mass of BH.

Ya. B. Zeldovich and I. D. Novikov (see Reference [139]) noticed that if cosmological expansion stops in some region, a black hole can be formed in this region within the cosmological horizon. This corresponds to strong deviation from general expansion and reflects strong inhomogeneity in the early universe. There are several mechanisms for such strong inhomogeneity and formation of Primordial Black Holes (PBHs) [140,141].

Here we outline the role of PBHs as a link in cosmoarcheological chain, connecting cosmological reflections of particle symmetry with observational data. We discuss the way in which the spectrum of PBHs reflects the properties of superheavy metastable particles and of phase transitions on inflationary and post-inflationary stages. We illustrate in Section 3.1 some mechanisms of PBH formation on the stage of dominance of superheavy particles and fields (Section 3.1.3) and from second order phase transition on the inflationary stage. An effective mechanism of BH formation during bubble nucleation provides a sensitive tool to probe the existence of cosmological first order phase transitions by PBHs (Section 3.3). The existence of stable remnants of PBH evaporation can strongly increase the sensitivity of such a probe, and we demonstrate this possibility in Section 3.4 on an example of gravitino production in PBH evaporation. Being formed within the cosmological horizon, PBHs seem to have masses much less than the mass of stars, constrained by the small size of the horizon in the very early universe.

However, if phase transition takes place in the inflationary stage, closed walls of practically any size can be formed, and their successive collapse can give rise to clouds of massive black holes, which can play the role of seeds for galaxies as discussed above in Section 2.4.2.

3.1. PBHs from Early Dust-Like Stages

The possibility of forming a black hole is highly improbable in a homogeneous expanding universe, since it implies metric fluctuations of order 1. For metric fluctuations distributed according to Gaussian law with dispersion

$$\langle \delta^2 \rangle \ll 1 \quad (16)$$

a probability for fluctuation of order 1 is determined by an exponentially small tail of the high amplitude part of this distribution. This probability can be further suppressed in the case of non-Gaussian fluctuations [142].

In the universe with equation of state

$$p = \gamma \epsilon \quad (17)$$

with numerical factor γ being in the range

$$0 \leq \gamma \leq 1 \quad (18)$$

the probability of forming a black hole from fluctuations within the cosmological horizon is given by [143]

$$W_{PBH} \propto \exp\left(-\frac{\gamma^2}{2\langle \delta^2 \rangle}\right) \quad (19)$$

This provides the exponential sensitivity of the PBH spectrum to the softening of the equation of state in the early universe ($\gamma \rightarrow 0$) or to the increase of ultraviolet part of the spectrum of density fluctuations ($\langle \delta^2 \rangle \rightarrow 1$). These phenomena can appear as a cosmological consequence of particle theory.

3.1.1. Dominance of Superheavy Particles in the Early Universe

Superheavy particles cannot be directly studied at accelerators. If they are stable, their existence can be probed by cosmological tests, but there is no direct link between astrophysical data and the existence of superheavy metastable particles with lifetime $\tau \ll 1$ s. It was first noticed in Reference [111] that the dominance of such particles in the universe before their decay at $t \leq \tau$ can result in the formation of PBHs, remaining in the universe after the particles decay and keeping some information on particle properties in their spectrum. This provided (though indirect) a possibility to probe the existence of such particles in astrophysical observations. Even the absence of observational evidence for PBHs is important. It puts restrictions on the allowed properties of superheavy metastable particles, which might form such PBHs on a stage of particle dominance, and thus constrains the parameters of models predicting these particles.

After reheating, at

$$T < T_0 = rm \quad (20)$$

particles with mass m and relative abundance $r = n/n_r$ (where n is the frozen out concentration of particles and n_r is the concentration of relativistic species) must dominate in the universe before their decay. Dominance of these nonrelativistic particles at $t > t_0$, where

$$t_0 = \frac{m_{pl}}{T_0^2} \quad (21)$$

corresponds to a dust-like stage with equation of state $p = 0$, at which particle density fluctuations grow as

$$\delta(t) = \frac{\delta\rho}{\rho} \propto t^{2/3} \quad (22)$$

and the development of gravitational instability results in the formation of gravitationally-bound systems which decouple at

$$t \sim t_f \approx t_i \delta(t_i)^{-3/2} \quad (23)$$

from general cosmological expansion, when $\delta(t_f) \sim 1$ for fluctuations entering the horizon at $t = t_i > t_0$ with amplitude $\delta(t_i)$.

The formation of these systems can result in black hole formation, either immediately after the system decouples from expansion or as a result of the evolution of the initially formed nonrelativistic gravitationally-bound system.

3.1.2. Direct PBH Formation

If density fluctuation is especially homogeneous and isotropic, it directly collapses to BH as soon as the amplitude of fluctuation grows to 1 and the system decouples from expansion. A probability for direct BH formation in the collapse of such homogeneous and isotropic configurations gives minimal estimation of BH formation in the dust-like stage.

This probability was calculated in Reference [111] with the use of the following arguments. In the period $t \sim t_f$, when fluctuation decouples from expansion, its configuration is defined by averaged density ρ_1 , size r_1 , deviation from sphericity s , and by inhomogeneity u of internal density distribution within the fluctuation. Having decoupled from expansion, the configuration contracts and the minimal size to which it can contract is

$$r_{min} \sim sr_1 \quad (24)$$

being determined by a deviation from sphericity

$$s = \max\{|\gamma_1 - \gamma_2|, |\gamma_1 - \gamma_3|, |\gamma_2 - \gamma_3|\} \quad (25)$$

where γ_1 , γ_2 , and γ_3 define a deformation of configuration along its three main orthogonal axes. It was first noticed in Reference [111] that in order to form a black hole as a result of such a contraction it is sufficient that the configuration returns to the size

$$r_{min} \sim r_g \sim t_i \sim \delta(t_i)r_1 \quad (26)$$

which had the initial fluctuation $\delta(t_i)$ when it entered the horizon at cosmological time t_i . If

$$s \leq \delta(t_i) \quad (27)$$

the configuration is sufficiently isotropic to concentrate its mass in the course of collapse within its gravitational radius, but such a concentration also implies sufficient homogeneity of configuration. Density gradients can result in gradients of pressure, which can prevent collapse to BH. This effect does not take place for the contracting collisionless gas of weakly interacting massive particles, but due to the inhomogeneity of collapse, the particles which have already passed the caustics can free stream beyond the gravitational radius before the whole mass is concentrated within it. Collapse of nearly spherically symmetric dust configuration is described by the Tolman solution. Its analysis [110,112,144,145] has provided a constraint on the inhomogeneity $u = \delta\rho_1/\rho_1$ within the configuration. It was shown that for both collisionless and interacting particles, the condition

$$u < \delta(t_i)^{3/2} \quad (28)$$

is sufficient for the configuration to contract within its gravitational radius.

The probability of direct BH formation is then determined by a product of probability for sufficient initial sphericity W_s and homogeneity W_u of configuration, which is determined by the phase space for such configurations. In a calculation of W_s , one should take into account that the condition (27) implies

five conditions for independent components of the tensor of deformation before its diagonalization (two conditions for three diagonal components to be close to each other, and three conditions for nondiagonal components to be small). Therefore, the probability of sufficient sphericity is given by [110–112,144,145]

$$W_s \sim \delta(t_i)^5 \quad (29)$$

and together with the probability for sufficient homogeneity

$$W_u \sim \delta(t_i)^{3/2} \quad (30)$$

results in the strong power-law suppression of probability for direct BH formation

$$W_{PBH} = W_s \cdot W_u \sim \delta(t_i)^{13/2} \quad (31)$$

Though this calculation was originally done in References [110–112,144,145] for Gaussian distribution of fluctuations, it does not imply a specific form of the high amplitude tail of this distribution, and thus should not change strongly in a case of non-Gaussian fluctuations [142].

The mechanism [1,2,110–112,144,145] is effective for the formation of PBHs with mass in an interval

$$M_0 \leq M \leq M_{bhmax} \quad (32)$$

The minimal mass corresponds to the mass within the cosmological horizon in the period $t \sim t_0$, when particles start to dominate in the universe and it is equal to [1,2,110–112,144,145]

$$M_0 = \frac{4\pi}{3} \rho t_0^3 \approx m_{pl} \left(\frac{m_{pl}}{rm} \right)^2 \quad (33)$$

The maximal mass is indirectly determined by the condition

$$\tau = t(M_{bhmax}) \delta(M_{bhmax})^{-3/2} \quad (34)$$

that fluctuation in the considered scale M_{bhmax} , entering the horizon at $t(M_{bhmax})$ with an amplitude $\delta(M_{bhmax})$, can manage to grow up to nonlinear stage, decouple, and collapse before particles decay at $t = \tau$. For scale-invariant spectrum $\delta(M) = \delta_0$, the maximal mass is given by [114]

$$M_{bhmax} = m_{pl} \frac{\tau}{t_{pl}} \delta_0^{-3/2} = m_{pl}^2 \tau \delta_0^{-3/2} \quad (35)$$

The probability, given by Equation (31), is also appropriate for the formation of PBHs in the dust-like preheating stage after inflation [1,2,146]. The simplest example of such a stage can be given by the use of a model of a homogeneous massive scalar field [1,2]. Slow rolling of the field in the period $t \ll 1/m$ (where m is the mass of the field) provides a chaotic inflation scenario, while at $t > 1/m$, the field oscillates with period $1/m$. Coherent oscillations of the field correspond to an average over a period of oscillations in a dust-like equation of state $p = 0$, at which gravitational instability can develop. The minimal mass in this case corresponds to the Jeans mass of scalar field, while the maximal mass is also determined by the condition that fluctuation grows and collapses before the scalar field decays and reheats the universe.

The probability $W_{PBH}(M)$ determines the fraction of total density

$$\beta(M) = \frac{\rho_{PBH}(M)}{\rho_{tot}} \approx W_{PBH}(M) \quad (36)$$

corresponding to PBHs with mass M . For $\delta(M) \ll 1$, this fraction (given by Equation 31) is small. This means that the bulk of particles do not collapse directly into black holes, but form

gravitationally-bound systems. The evolution of these systems can give a much larger amount of PBHs, but it strongly depends on particle properties.

3.1.3. Evolutional Formation of PBHs

Superweakly interacting particles form gravitationally bound systems of collisionless gas, which resemble modern galaxies with collisionless gas of stars. Such a system can finally collapse to a black hole, but energy dissipation within it—and consequently, its evolution—is a relatively slow process [1,2,147]. The evolution of these systems is dominantly determined by the evaporation of particles, which gain velocities exceeding the parabolic velocity of the system. In the case of binary collisions, the evolution timescale can be roughly estimated [1,2,147] as

$$t_{ev} = \frac{N}{\ln N} t_{ff} \quad (37)$$

for a gravitationally-bound system of N particles, where the free fall time t_{ff} for a system with density ρ is $t_{ff} \approx (4\pi G\rho)^{-1/2}$. This time scale can be shorter due to collective effects in collisionless gas [148] and at large N can be on the order of

$$t_{ev} \sim N^{2/3} t_{ff} \quad (38)$$

However, since the free fall time scale for gravitationally-bound systems of collisionless gas is on the order of cosmological time t_f for the period when these systems are formed, even in the latter case the particles should be very long-living ($\tau \ll t_f$) to form black holes in such a slow evolutionary process.

The evolutionary time scale is much smaller for gravitationally-bound systems of superheavy particles interacting with light relativistic particles and radiation. Such systems have analogy with stars, in which evolution time scale is defined by energy loss by radiation. An example of such particles is superheavy color octet fermions of asymptotically free SU(5) model [149] or magnetic monopoles of GUT models. Having decoupled from expansion, frozen out particles and antiparticles can annihilate in gravitationally-bound systems, but detailed numerical simulation [150] has shown that annihilation cannot prevent the collapse of the majority of mass, and the timescale of collapse does not exceed the cosmological time of the period when the systems are formed.

3.2. Spikes from Phase Transitions in the Inflationary Stage

Scale non-invariant spectrum of fluctuations—in which the amplitude of small scale fluctuations is enhanced—can be another factor, increasing the probability of PBH formation. The simplest functional form of such a spectrum is represented by a blue spectrum with a power law dispersion

$$\langle \delta^2(M) \rangle \propto M^{-k} \quad (39)$$

with the amplitude of fluctuations growing at $k > 0$ to small M . The realistic account for the existence of other scalar fields together with inflaton in the period of inflation can give rise to spectra with distinguished scales, determined by the parameters of the considered fields and their interaction.

In the chaotic inflation scenario, interaction of a Higgs field ϕ with an inflaton η can give rise to phase transitions in the inflationary stage if this interaction induces positive mass term $+\frac{v^2}{2}\eta^2\phi^2$. When in the course of slow rolling, the amplitude of an inflaton decreases below a certain critical value $\eta_c = m/v$, the mass term in Higgs potential

$$V(\phi, \eta) = -\frac{m_\phi^2}{2}\phi^2 + \frac{\lambda_\phi}{4}\phi^4 + \frac{v^2}{2}\eta^2\phi^2 \quad (40)$$

changes sign, and phase transition takes place. Such phase transitions in the inflationary stage lead to the appearance of a characteristic spike in the spectrum of initial density perturbations. These spike-like perturbations, on scales that cross the horizon ($60 \geq N \geq 1$), e -fold before the end of inflation and

reenter the horizon during the radiation or dust-like era and could in principle collapse to form primordial black holes. The possibility of such spikes in the chaotic inflation scenario was first pointed out in Reference [151] and realized in Reference [152] as a mechanism of PBH formation for the model of horizontal unification [36–39].

For the vacuum expectation value of a Higgs field

$$\langle \phi \rangle = \frac{m}{\lambda} = v \quad (41)$$

and $\lambda \sim 10^{-3}$, the amplitude δ of a spike in the spectrum of density fluctuations, generated in phase transition in the inflationary stage is given by [152]

$$\delta \approx \frac{4}{9s} \quad (42)$$

with

$$s = \sqrt{\frac{4}{9} + \kappa 10^5 \left(\frac{v}{m_{pl}} \right)^2} - \frac{3}{2} \quad (43)$$

where $\kappa \sim 1$.

If phase transition takes place at e -folding N before the end of inflation, the spike re-enters the horizon at the radiation dominance (RD) stage and forms a Black hole of mass

$$M \approx \frac{m_{Pl}^2}{H_0} \exp\{2N\} \quad (44)$$

where H_0 is the Hubble constant in the period of inflation.

If the spike re-enters the horizon in the matter dominance (MD) stage, it should form black holes of mass

$$M \approx \frac{m_{Pl}^2}{H_0} \exp\{3N\}. \quad (45)$$

3.3. First Order Phase Transitions as a Source of Black Holes in the Early Universe

First order phase transitions go through bubble nucleation, recalling the common example of boiling water. The simplest way to describe first order phase transitions with bubble creation in the early universe is based on a scalar field theory with two non-degenerated vacuum states. Being stable at a classical level, the false vacuum state decays due to quantum effects, leading to the nucleation of bubbles of true vacuum and their subsequent expansion [153]. The potential energy of the false vacuum is converted into the kinetic energy of bubble walls, thus making them highly relativistic in a short time. The bubble expands until it collides with another one. As it was shown in References [154,155], a black hole may be created in a collision of several bubbles. The probability of the collision of two bubbles is much higher. The opinion of the absence of black holes (BHs) in such processes was based on strict conservation of the original $O(2,1)$ symmetry. As shown in References [113,156,157], there are ways to break it. Firstly, radiation of scalar waves indicates increasing entropy, and hence the permanent breaking of the symmetry during bubble collision. Secondly, the vacuum decay due to thermal fluctuation does not possess this symmetry from the beginning. The investigations [113,156,157] have shown that BH can also be created with a probability of order unity in collisions of only two bubbles. This initiates an enormous production of BH that leads to essential cosmological consequences discussed below.

Inflation models ended by a first order phase transition hold a dignified position in the modern cosmology of the early universe (see for example [158–164]). The interest in these models is due to the fact that such models are able to generate the observed large-scale voids as remnants of the primordial bubbles for which the characteristic wavelengths are several tens of Mpc [163,164]. A detailed analysis

of a first order phase transition in the context of extended inflation can be found in Reference [165]. Hereafter, we will be interested only in a final stage of inflation when the phase transition is completed. Remember that a first order phase transition is considered completed immediately after establishing the true vacuum percolation regime. Such a regime is established approximately when at least one bubble per unit Hubble volume is nucleated. Accurate computation [165] shows that first order phase transition is successful if the following condition is valid:

$$Q \equiv \frac{4\pi}{9} \left(\frac{\Gamma}{H^4} \right)_{t_{end}} = 1 \quad (46)$$

Here Γ is the bubble nucleation rate. In the framework of first order inflation models, the filling of all space by true vacuum takes place due to bubble collisions, nucleated at the final moment of exponential expansion. The collisions between such bubbles occur when they have comoving spatial dimension less than or equal to the effective Hubble horizon H_{end}^{-1} at the transition epoch. If we take $H_0 = 100 h \text{Km/s/Mpc}$ in $\Omega = 1$ universe, the comoving size of these bubbles is approximately $10^{-21} h^{-1} \text{Mpc}$. In the standard approach it is believed that such bubbles are rapidly thermalized without leaving a trace in the distribution of matter and radiation. However, in the previous section it was shown that for any realistic parameters of the theory, the collision between only two bubbles leads to BH creation with a probability close to 100%. The mass of this BH is given by [113,156,157]

$$M_{BH} = \gamma_1 M_{bub} \quad (47)$$

where $\gamma_1 \simeq 10^{-2}$ and M_{bub} is the mass that could be contained in the bubble volume at the epoch of collision in the condition of the full thermalization of bubbles. The discovered mechanism leads to a new direct possibility of PBH creation at the epoch of reheating in first order inflation models. In the standard picture, PBHs are formed in the early universe if density perturbations are sufficiently large, and the probability of PBH formation from small post-inflation initial perturbations is suppressed (see Section 3.1). A completely different situation takes place at the final epoch of the first order inflation stage; namely, collision between bubbles of Hubble size in the percolation regime leads to copious PBH formation with masses

$$M_0 = \gamma_1 M_{end}^{hor} = \frac{\gamma_1}{2} \frac{m_{pl}^2}{H_{end}} \quad (48)$$

where M_{end}^{hor} is the mass of the Hubble horizon at the end of inflation. According to (47), the initial mass fraction of this PBH is given by $\beta_0 \approx \gamma_1/e \approx 6 \times 10^{-3}$. For example, for a typical value of $H_{end} \approx 4 \times 10^{-6} m_{pl}$, the initial mass fraction β is contained in PBHs with mass $M_0 \approx 1 \text{ g}$.

In general, the Hawking evaporation of mini BHs [166] could give rise to a variety of possible end states. It is generally assumed that evaporation proceeds until the PBH vanishes completely [167], but there are various arguments against this proposal (see References [168–171]). If one supposes that BH evaporation leaves a stable relic, then it is natural to assume that it has a mass of order $m_{rel} = km_{pl}$, where $1 \leq k \leq 10^2$. We can investigate the consequences of PBH formation at the percolation epoch after first order inflation, supposing that the stable relic is a result of its evaporation. As it follows from the above consideration, the PBHs are preferentially formed with a typical mass M_0 at a single time t_1 . Hence, the total density ρ at this time is

$$\rho(t_1) = \rho_\gamma(t_1) + \rho_{PBH}(t_1) = \frac{3(1-\beta_0)}{32\pi t_1^2} m_{pl}^2 + \frac{3\beta_0}{32\pi t_1^2} m_{pl}^2 \quad (49)$$

where β_0 denotes the fraction of the total density corresponding to PBHs in the period of their formation t_1 . The evaporation time scale can be written in the following form

$$\tau_{BH} = \frac{M_0^3}{g_* m_{pl}^4} \quad (50)$$

where g_* is the number of effective massless degrees of freedom.

Let us derive the density of PBH relics. There are two distinct possibilities to consider.

The universe is still radiation dominated (RD) at τ_{BH} . This situation will hold if the following condition is valid: $\rho_{BH}(\tau_{BH}) < \rho_\gamma(\tau_{BH})$. It is possible to rewrite this condition in terms of Hubble constant at the end of inflation

$$\frac{H_{end}}{m_{pl}} > \beta_0^{5/2} g_*^{-1/2} \simeq 10^{-6} \quad (51)$$

Taking the present radiation density fraction of the universe to be $\Omega_{\gamma_0} = 2.5 \times 10^{-5} h^{-2}$ (h being the Hubble constant in the units of $100 \text{ km} \cdot \text{s}^{-1} \text{ Mpc}^{-1}$), and using the standard values for the present time and time when the density of matter and radiation become equal, we find the contemporary densities fraction of relics

$$\Omega_{rel} \approx 10^{26} h^{-2} k \left(\frac{H_{end}}{m_{pl}} \right)^{3/2} \quad (52)$$

It is easily to see that relics overclose the universe ($\Omega_{rel} \gg 1$) for any reasonable k and $H_{end} > 10^{-6} m_{pl}$.

The second case takes place if the universe becomes PBHs dominated at period $t_1 < t_2 < \tau_{BH}$. This situation is realized under the condition $\rho_{BH}(t_2) < \rho_\gamma(t_2)$, which can be rewritten in the form

$$\frac{H_{end}}{m_{pl}} < 10^{-6} \quad (53)$$

The present day relics density fraction takes the form

$$\Omega_{rel} \approx 10^{28} h^{-2} k \left(\frac{H_{end}}{m_{pl}} \right)^{3/2} \quad (54)$$

Thus, the universe is not overclosed by relics, only if the following condition is valid

$$\frac{H_{end}}{m_{pl}} \leq 2 \times 10^{-19} h^{4/3} k^{-2/3} \quad (55)$$

This condition implies that the masses of PBHs created at the end of inflation have to be larger then

$$M_0 \geq 10^{11} \text{ g} \cdot h^{-4/3} \cdot k^{2/3} \quad (56)$$

On the other hand, there are a number of well-known cosmological and astrophysical limits [172–178] which prohibit the creation of PBHs in the mass range (56) with initial fraction of mass density close to $\beta_0 \approx 10^{-2}$.

So, one has to conclude that the effect of the false vacuum bag mechanism of PBH formation makes the coexistence of stable remnants of PBH evaporation with the first order phase transitions at the end of inflation impossible.

3.4. PBH Evaporation as Universal Particle Accelerator

Presently, there is no observational evidence proving the existence of PBHs. However, even the absence of PBHs provides a very sensitive theoretical tool to study the physics of the early universe. PBHs represent a nonrelativistic form of matter, and their density decreases with scale factor

a as $\propto a^{-3} \propto T^3$, while the total density is $\propto a^{-4} \propto T^4$ in the period of radiation dominance (RD). Being formed within the horizon, a PBH of mass M can be formed not earlier than at

$$t(M) = \frac{M}{m_{pl}} t_{pl} = \frac{M}{m_{pl}^2} \quad (57)$$

If they are formed in the RD stage, the smaller the masses of PBHs, the larger becomes their relative contribution to the total density in the modern MD stage. Therefore, even the modest constraint for PBHs of mass M on their density

$$\Omega_{PBH}(M) = \frac{\rho_{PBH}(M)}{\rho_c} \quad (58)$$

in units of critical density $\rho_c = 3H^2/(8\pi G)$ from the condition that their contribution $\alpha(M)$ into the the total density

$$\alpha(M) \equiv \frac{\rho_{PBH}(M)}{\rho_{tot}} = \Omega_{PBH}(M) \quad (59)$$

for $\rho_{tot} = \rho_c$ does not exceed the density of dark matter

$$\alpha(M) = \Omega_{PBH}(M) \leq \Omega_{DM} = 0.23 \quad (60)$$

converts into a severe constraint on this contribution

$$\beta \equiv \frac{\rho_{PBH}(M, t_f)}{\rho_{tot}(t_f)} \quad (61)$$

in the period t_f of their formation. If formed in the RD stage at $t_f = t(M)$ (given by 57), which corresponds to the temperature $T_f = m_{pl} \sqrt{m_{pl}/M}$, PBHs contribute to the total density in the end of the RD stage at t_{eq} , corresponding to $T_{eq} \approx 1$ eV, by a factor of $a(t_{eq})/a(t_f) = T_f/T_{eq} = m_{pl}/T_{eq} \sqrt{m_{pl}/M}$ larger than in the period of their formation. The constraint on $\beta(M)$, following from Equation (60) is then given by

$$\beta(M) = \alpha(M) \frac{T_{eq}}{m_{pl}} \sqrt{\frac{M}{m_{pl}}} \leq 0.23 \frac{T_{eq}}{m_{pl}} \sqrt{\frac{M}{m_{pl}}} \quad (62)$$

The possibility of PBH evaporation, revealed by S. Hawking [166], strongly influences the effects of PBHs. In the strong gravitational field near the gravitational radius r_g of PBH, a quantum effect of the creation of particles with momentum $p \sim 1/r_g$ is possible. Due to this effect, PBHs turn out to be a black body source of particles with temperature (in the units $\hbar = c = k = 1$)

$$T = \frac{1}{8\pi GM} \approx 10^{13} \text{GeV} \frac{1\text{g}}{M} \quad (63)$$

The BH evaporation timescale is $\tau_{BH} \sim M^3/m_{pl}^4$ (see Equation (50) and discussion in previous section), and at $M \leq 10^{14}$ g is less than the age of the universe. Such PBHs cannot survive to the present time, and their magnitude Equation (60) should be re-defined and has the meaning of contribution to the total density in the moment of PBH evaporation. For PBHs formed in the RD stage and evaporated in the RD stage at $t < t_{eq}$, the relationship Equation (62) between $\beta(M)$ and $\alpha(M)$ is given by [110,179]:

$$\beta(M) = \alpha(M) \frac{m_{pl}}{M} \quad (64)$$

The relationship between $\beta(M)$ and $\alpha(M)$ has a more complicated form if PBHs are formed in early dust-like stages [1,110,144,180], or if such stages take place after PBH formation [1,180]. The relative contribution of PBHs to total density does not grow in the dust-like stage, and the relationship between $\beta(M)$ and $\alpha(M)$ depends on the details of a considered model. Minimal model independent factor $\alpha(M)/\beta(M)$ follows from the account for enhancement, taking place only during the RD stage between the first second of expansion and the end of the RD stage at t_{eq} , since radiation dominance in this period is supported by observations of light element abundance and the spectrum of CMB [1,110,144,180].

Effects of PBH evaporation make astrophysical data much more sensitive to the existence of PBHs. Constraining the abundance of primordial black holes can lead to invaluable information on cosmological processes, particularly as they are probably the only viable probe for the power spectrum on very small scales which remain far from the Cosmological Microwave Background (CMB) and Large Scale Structures (LSS) sensitivity ranges. To date, only PBHs with initial masses between $\sim 10^9$ g and $\sim 10^{16}$ g have led to stringent limits (see References [110,168,181,182]) from consideration of the entropy per baryon, the deuterium destruction, the ^4He destruction, and the cosmic-rays currently emitted by the Hawking process [166]. The existence of light PBHs should lead to important observable constraints, either through the direct effects of the evaporated particles (for initial masses between 10^{14} g and 10^{16} g) or through the indirect effects of their interaction with matter and radiation in the early universe (for PBH masses between 10^9 g and 10^{14} g). In these constraints, the effects taken into account are those related to known particles. However, since the evaporation products are created by the gravitational field, any quantum with a mass lower than the black hole temperature should be emitted, independently of the strength of its interaction. This could provide a copious production of superweakly interacting particles that cannot be in equilibrium with the hot plasma of the very early universe. This makes evaporating PBHs a unique source of all the species which can exist in the universe.

Following References [1,2,98,180] and [183,184] (but in a different framework and using more stringent constraints), limits on the mass fraction of black holes at the time of their formation ($\beta \equiv \rho_{PBH}/\rho_{tot}$) were derived in Reference [185] using the production of gravitinos during the evaporation process. Depending on whether gravitinos are expected to be stable or metastable, the limits are obtained using the requirement that they do not overclose the universe and that the formation of light nuclei by the interactions of ^4He nuclei with nonequilibrium flux of D, T, ^3He and ^4He does not contradict the observations. This approach is more constraining than the usual study of photo-dissociation induced by photons–photinos pairs emitted by decaying gravitinos. This opened a new window for the upper limits on β below 10^9 g, and correspondingly on various mechanisms of PBH formation [185]. Some other aspects of PBH formation and effects are discussed in References [186–188].

4. Dark Matter from Flavor Symmetry

4.1. Symmetry of Known Families

The existence and observed properties of the three known quark-lepton families appeal to the broken $SU(3)_H$ family symmetry [36–38], which should be involved in the extension of the standard model. This provides the possibility of *horizontal unification* in the “bottom-up” approach to the unified theory [39]. Even in its minimal implementation, the model of *horizontal unification* can reproduce the main necessary elements of modern cosmology. It provides the physical mechanisms for inflation and baryosynthesis and offers a unified description of candidates for Cold, Warm, Hot, and Unstable Dark Matter. Methods of cosmoparticle physics [1,2] have provided the complete test of this model. Here we discuss the possibilities of linking the physical basis of modern cosmology to the parameters of broken family symmetry.

4.1.1. Horizontal Hierarchy

The approach of References [36–39] (and its revival in References [189–191]) follows the concept of local gauge symmetry $SU(3)_H$, first proposed by Chkareuli [192]. Under the action of this symmetry, the left-handed quarks and leptons transform as $SU(3)_H$ triplets and the right-handed quarks and leptons as antitriplets. Their mass term transforms as $3 \otimes 3 = 6 \otimes \bar{3}$, and therefore, can only form as a result of horizontal symmetry breaking.

This approach can be trivially extended to the case of n generations, assuming the proper $SU(n)$ symmetry. For three generations, the choice of horizontal symmetry $SU(3)_H$ is the only possible choice because the orthogonal and vector-like gauge groups cannot provide different representations for the left- and right-handed fermion states.

In the considered approach, the hypothesis that the structure of the mass matrix is determined by the structure of horizontal symmetry breaking—i.e., the structure of the vacuum expectation values of horizontal scalars carrying the $SU(3)_H$ breaking—is justified.

The mass hierarchy between generations is related to the hypothesis of a hierarchy of such symmetry breaking. This hypothesis is called the hypothesis of horizontal hierarchy (HHH) [193–195].

The model is based on the gauge $SU(3)_H$ flavor symmetry, which is additional to the symmetry of the standard model. It means that there exist eight heavy horizontal gauge bosons, and there are three multiplets of heavy Higgs fields $\zeta_{ij}^{(n)}$ (i, j -family indexes, $n = 1, 2, 3$) in nontrivial (sextet or triplet) representations of $SU(3)_H$. These heavy Higgs bosons are singlets relative to electroweak symmetry, and don't have Yukawa couplings with ordinary light fermions. They have direct coupling to heavy fermions. The latter are singlets relative to electroweak symmetry. Ordinary Higgs ϕ of the standard model is singlet relative to $SU(3)_H$. It couples left-handed light fermions f_L^i to their heavy right-handed partners F_R^i , which are coupled by heavy Higgs multiplets ζ_{ij} with heavy left-handed states F_L^j . Heavy left-handed states F_L^j are coupled to right-handed light states f_R^j by a singlet scalar Higgs field η , which is singlet both relative to $SU(3)_H$ and electroweak group of symmetry. The described succession of transitions realizes the Dirac see-saw mechanism, which reproduces the mass matrix m_{ij} of ordinary light quarks and charged leptons f due to mixing with their heavy partners F . This fixes the ratio of vacuum expectation values of heavy Higgs fields, leaving their absolute value as the only main free parameter, which is determined from the analysis of physical, astrophysical, and cosmological consequences.

The $SU(3)_H$ flavor symmetry should be chiral in order to eliminate the flavor symmetric mass term. The condition of absence of anomalies implies heavy partners of light neutrinos, and the latter acquire mass by Majorana *see-saw* mechanism. The natural absence of triple couplings in the heavy Higgs potentials, which do not appear as radiative effects of any other (gauge or Yukawa) interaction, supports additional global U(1) symmetry, which can be associated with Peccei–Quinn symmetry and whose breaking results in the Nambu–Goldstone scalar field, which shares the properties of axion, Majoron, and singlet familon.

4.1.2. Horizontal Unification

The model provides a complete test (in which its simplest implementation is already ruled out) in a combination of laboratory tests and analysis of cosmological and astrophysical effects. The latter include the study of the effect of radiation of axions on the processes of stellar evolution, the study of the impact of the effects of primordial axion fields and massive unstable neutrinos on the dynamics of the formation of the large-scale structure of the universe, as well as the analysis of the mechanisms of inflation and baryosynthesis based on the physics of the hidden sector of the model.

The model results in physically self-consistent inflationary scenarios with dark matter in the baryon-asymmetric universe. In these scenarios, all steps of cosmological evolution correspond quantitatively to the parameters of particle theory. The physics of the inflaton correspond to the Dirac *see-saw* mechanism of the generation of the mass of quarks and charged leptons, and the leptogenesis

of baryon asymmetry is based on the physics of Majorana neutrino masses. The parameters of axion cold dark matter (CDM), as well as the masses and lifetimes of neutrinos, correspond to the hierarchy of breaking of the $SU(3)_H$ symmetry of families.

4.2. Stable Charged Constituents of Dark Atoms

New stable particles may possess new U(1) gauge charges and bind by Coulomb-like forces in composite dark matter species. Such dark atoms would look nonluminous, since they radiate invisible light of U(1) photons. Historically, mirror matter (see Section 2.2.4 and References [1,63] for review and references) seems to be the first example of such a nonluminous atomic dark matter.

However, it turned out that the possibility of new stable charged leptons and quarks is not completely excluded, and Glashow's tera-helium [97] has offered a new solution for dark atoms of dark matter. Tera-U-quarks with electric charge $+2/3$ formed stable (UUU) $+2$ charged "clusters" that formed with two -1 charged tera-electrons E neutral [(UUU)EE] tera-helium "atoms" that behaved like Weakly Interacting Massive Particles (WIMPs). The main problem for this solution was to suppress the abundance of positively charged species bound with ordinary electrons, which behave as anomalous isotopes of hydrogen or helium. This problem turned out to be unresolvable [84], since the model [97] predicted stable tera-electrons E^- with charge -1 . As soon as primordial helium is formed in the Standard Big Bang Nucleosynthesis (SBBN), it captures all the free E^- in the positively charged $(HeE)^+$ ion, preventing any further suppression of positively charged species. Therefore, in order to avoid the overproduction of anomalous isotopes, stable particles with charge -1 (and corresponding antiparticles) should be absent, so that stable negatively charged particles should have charge -2 only.

Elementary particle frames for heavy stable -2 charged species are provided by: (a) stable "antibaryons" $\bar{U}\bar{U}\bar{U}$ formed by anti-U fourth generation quarks [88–90,196,197]; (b) Leptons from Almost Commutative geometry (AC leptons) [87,90], predicted in the extension [87] of the standard model, based on the approach of almost-commutative geometry [198]; (c) Technileptons and anti-technibaryons [199] in the framework of walking technicolor models (WTC) [200–205]; (d) Finally, stable charged clusters $\bar{u}_5\bar{u}_5\bar{u}_5$ of (anti)quarks \bar{u}_5 of the fifth family can follow from the approach, unifying spins and charges [206].

Since all these models also predict corresponding $+2$ charge antiparticles, the cosmological scenario should provide a mechanism for their suppression, which can naturally take place in the asymmetric case, corresponding to an excess of -2 charge species, O^{--} . Then, their positively charged antiparticles can effectively annihilate in the early universe.

If new stable species belong to non-trivial representations of the electroweak SU(2) group, sphaleron transitions at high temperatures can provide the relationship between baryon asymmetry and an excess of -2 charge stable species, as was demonstrated in the case of WTC in References [199,207–211].

4.2.1. Problem of Tera-Fermion Composite Dark Matter

Glashow's Tera-helium universe was the first inspiring example of the composite dark matter scenario. $SU(3)_c \times SU(2) \times SU(2)' \times U(1)$ gauge model [97] aimed to explain the origin of the neutrino mass and to solve the problem of strong CP-violation in QCD. New extra $SU(2)'$ symmetry acts on three heavy generations of tera-fermions linked with the light fermions by CP' transformation. $SU(2)'$ symmetry breaking at the TeV scale makes tera-fermions much heavier than their light partners. Tera-fermion mass spectrum is the same as for light generations, but all the masses are scaled by the same factor of about 10^6 . Thus, the masses of the lightest heavy particles are in the *tera*-eV (TeV) range, explaining their name.

Glashow's model [97] takes into account that very heavy quarks Q (or antiquarks \bar{Q}) can form bound states with other heavy quarks (or antiquarks) due to their Coulomb-like QCD attraction, and the binding energy of these states substantially exceeds the binding energy of QCD confinement. Then, stable (QQq) and $(QQ\bar{Q})$ baryons can exist.

According to Reference [97], primordial heavy quark U and heavy electron E are stable and may form a neutral ($UUUEE$) “atom” with a (UUU) hadron as nucleus and two E^- s as “electrons”. The gas of such “tera-helium atoms” was proposed in Reference [97] as a candidate for a WIMP-like dark matter.

The problem of such a scenario is the inevitable presence of “products of incomplete combustion”, and the necessity to decrease their abundance.

Unfortunately, as was shown in Reference [84], this picture of a Tera-helium universe cannot be realized.

When ordinary ${}^4\text{He}$ is formed in Big Bang Nucleosynthesis, it binds all the free E^- into positively charged (${}^4\text{He}E^-$)⁺ “ions”. This creates a Coulomb barrier for any successive E^-E^+ annihilation or any effective EU binding. It removes the possibility of suppressing the abundance of unwanted tera-particle species (like (eE^+), (${}^4\text{He}Ee$), etc.). For instance, the remaining abundance of (eE^+) and (${}^4\text{He}E^-e$) exceeds the terrestrial upper limit for anomalous hydrogen by 27 orders of magnitude [84].

4.2.2. Composite Dark Matter from Almost Commutative Geometry

The AC-model is based on the specific mathematical approach of unifying general relativity, quantum mechanics, and gauge symmetry [87,198]. This realization naturally embeds the standard model, both reproducing its gauge symmetry and Higgs mechanism with the prediction of a Higgs boson mass. The AC model is in some sense alternative to SUSY, GUT, and superstring extensions of the standard model. The AC-model [87] extends the fermion content of the Standard model by two heavy particles— $SU(2)$ electro-weak singlets, with opposite electromagnetic charges. Each of them has its own antiparticle. Having no other gauge charges of the standard model, these particles (AC-fermions) behave as heavy stable leptons with charges $-2e$ and $+2e$, called A^{--} and C^{++} , respectively.

Similar to the Tera-helium Universe, AC-lepton relics from intermediate stages of a multi-step process towards a final (AC) atom formation must survive in the present universe. In spite of the assumed excess of particles (A^{--} and C^{++}), the abundance of relic antiparticles (\bar{A}^{++} and \bar{C}^{--}) is not negligible. There may also be a significant fraction of A^{--} and C^{++} which remains unbound after the recombination process of these particles into (AC) atoms took place. As soon as ${}^4\text{He}$ is formed in Big Bang nucleosynthesis, the primordial component of free anion-like AC-leptons (A^{--}) is mostly trapped in the first three minutes into a neutral O-helium atom ${}^4\text{He}^{++}A^{--}$. O-helium is able to capture free C^{++} , creating (AC) atoms and releasing ${}^4\text{He}$ back. In the same way, the annihilation of antiparticles speeds up. C^{++} -O-helium reactions stop when their timescale exceeds a cosmological time, leaving O-helium and C^{++} relics in the universe. The catalytic reaction of O-helium with C^{++} in the dense matter bodies provides successive (AC) binding that suppresses terrestrial anomalous isotope abundance below the experimental upper limit. Due to the screened charge of AC-atoms, they have WIMP-like interaction with ordinary matter. Such WIMPs are inevitably accompanied by a tiny component of nuclear interacting O-helium.

4.2.3. Stable Charged Techniparticles in Walking Technicolor

The minimal walking technicolor model [200–205] has two techniquarks—i.e., up U and down D —that transform under the adjoint representation of a $SU(2)$ technicolor gauge group. The six Goldstone bosons UU , UD , DD , and their corresponding antiparticles carry a technibaryon number, since they are made of two techniquarks or two anti-techniquarks. This means that if there are no processes violating the technibaryon number, the lightest technibaryon will be stable.

The electric charges of UU , UD , and DD are given in general by $q + 1$, q , and $q - 1$, respectively, where q is an arbitrary real number. The model additionally requires the existence of a fourth family of leptons—i.e., a “new neutrino” ν' and a “new electron” ζ . Their electric charges are in terms of q , respectively, $(1 - 3q)/2$ and $(-1 - 3q)/2$.

There are three possibilities for a scenario of dark atoms of dark matter. The first one is to have an excess of $\bar{U}\bar{U}$ (charge -2). The technibaryon number TB is conserved, and therefore UU (or $\bar{U}\bar{U}$)

is stable. The second possibility is to have an excess of ζ that also has -2 charge and is stable, if ζ is lighter than ν' and technilepton number L' is conserved. In both cases, stable particles with -2 electric charge have substantial relic densities and can capture ${}^4\text{He}^{++}$ nuclei to form a neutral techni-O-helium atom. Finally there is a possibility to have both L' and TB conserved. In this case, the dark matter would be composed of bound atoms (${}^4\text{He}^{++}\zeta^{--}$) and $(\zeta^{--}(UU)^{++})$. In the latter case, the excess of ζ^{--} should be larger than the excess of $(UU)^{++}$, so that WIMP-like $(\zeta^{--}(UU)^{++})$ is subdominant at the dominance of nuclear interacting techni-O-helium.

The technicolor and the Standard Model particles are in thermal equilibrium as long as the timescale of the weak (and color) interactions is smaller than the cosmological time. The sphalerons allow violation of TB , of baryon number B , of lepton number L , and L' , as long as the temperature of the universe exceeds the electroweak scale. It was shown in [199] that there is a balance between the excess of techni(anti)baryons, $(\bar{U}\bar{U})^{--}$, technileptons ζ^{--} , or of the both over the corresponding particles (UU and/or ζ^{++}), and the observed baryon asymmetry of the universe. It was also shown there are parameters of the model at which this asymmetry has proper sign and value, explaining the dark matter density.

4.2.4. Stable Particles of Fourth Generation Matter

Though precision data on the parameters of the standard model did not exclude [212] the existence of the fourth generation of quarks and leptons, the LHC data on the 125 GeV Higgs boson exclude its full strength coupling to fourth family fermions. However, since these fermions should have much larger mass than quarks and leptons of the three known families, it would be reasonable to assume that the main contribution in their mass generation comes from another, more heavy Higgs field. It leads to the suppression of their coupling to a 125 GeV Higgs boson. Then, the limits on the deviation of its production cross-section and probabilities of decay modes from the prediction of the Standard model convert in the constraints on this suppressed coupling [213]. The analysis of the application of the LHC results to the direct searches for stable fourth generation quarks and leptons, as well as of the precision SM data for suppressed Higgs couplings need special study.

The fourth generation follows from heterotic string phenomenology, and its difference from the three known light generations can be explained by a new conserved charge, possessed only by its quarks and leptons [67,80,88,196,214]. Strict conservation of this charge makes the lightest particle of the fourth family (neutrino) absolutely stable, but it was shown in References [67,80,214] that this neutrino cannot be the dominant form of dark matter. The same conservation law requires the lightest quark to be long living [88,196]. In principle, the lifetime of U can exceed the age of the universe if $m_U < m_D$ [88,196]. Provided that sphaleron transitions establish excess of \bar{U} , antiquarks at the observed baryon asymmetry ($\bar{U}\bar{U}\bar{U}$) can be formed and bound with ${}^4\text{He}$ in atom-like state of O-helium [88].

In the successive discussion of OHe dark matter, we generally do not specify the type of -2 charged particle, denoting it as O^{--} . However, one should note that the AC model does not provide OHe as the dominant form of dark matter, so that the quantitative features of the OHe-dominated universe are not related to this case.

5. Dark Atoms with Helium Shell

Here we concentrate on the properties of OHe atoms, their interaction with matter, and the qualitative picture of OHe cosmological evolution [87,88,199,209,215–217] and observable effects. We show from the following References [90,218] that the interaction of OHe with nuclei in underground detectors can explain the positive results of dark matter searches in DAMA/NaI (see for review Reference [69]) and DAMA/LIBRA [70] experiments by annual modulations of the radiative capture of O-helium, resolving the controversy between these results and the results of other experimental groups.

After it is formed in the Standard Big Bang Nucleosynthesis (SBBN), ${}^4\text{He}$ screens the excessive O^{--} charged particles in composite (${}^4\text{He}^{++}O^{--}$) O-helium (OHe) "atoms" [88].

In all the considered forms of O-helium, O^{--} behaves either as lepton or as a specific “heavy quark cluster” with strongly-suppressed hadronic interaction. Therefore, O-helium interaction with matter is determined by nuclear interaction of He . These neutral primordial nuclear interacting species can play the role of a nontrivial form of strongly interacting dark matter [219–227], giving rise to a Warmer than Cold dark matter scenario [207,208,215].

5.1. OHe Atoms and Their Interaction with Nuclei

The structure of an OHe atom follows from the general analysis of the bound states of O^{--} with nuclei.

Consider a simple model [228–230] in which the nucleus is regarded as a sphere with uniform charge density and in which the mass of the O^{--} is assumed to be much larger than that of the nucleus. Spin dependence is also not taken into account, so both the particle and nucleus are considered as scalars. Then, the Hamiltonian is given by

$$H = \frac{p^2}{2Am_p} - \frac{ZZ_0\alpha}{2R} + \frac{ZZ_0\alpha}{2R} \cdot \left(\frac{r}{R}\right)^2 \quad (65)$$

for short distances $r < R$ and

$$H = \frac{p^2}{2Am_p} - \frac{ZZ_0\alpha}{R} \quad (66)$$

for long distances $r > R$, where α is the fine structure constant, $R = d_n A^{1/3} \sim 1.2A^{1/3}/(200 \text{ MeV})$ is the nuclear radius, Z is the electric charge of the nucleus, and $Z_0 = 2$ is the electric charge of the negatively charged particle O^{--} . Since $Am_p \ll M_o$, the reduced mass is $1/m = 1/(Am_p) + 1/M_o \approx 1/(Am_p)$.

For small nuclei, the Coulomb binding energy is like in hydrogen atom and is given by

$$E_b = \frac{1}{2}Z^2Z_0^2\alpha^2 Am_p \quad (67)$$

For large nuclei, O^{--} is inside the nuclear radius and the harmonic oscillator approximation is valid for the estimation of the binding energy

$$E_b = \frac{3}{2} \left(\frac{ZZ_0\alpha}{R} - \frac{1}{R} \left(\frac{ZZ_0\alpha}{Am_p R} \right)^{1/2} \right) \quad (68)$$

For the intermediate regions between these two cases with the use of trial function of the form $\psi \sim e^{-\gamma r/R}$, variational treatment of the problem [228–230] gives

$$E_b = \frac{1}{Am_p R^2} F(ZZ_0\alpha Am_p R) \quad (69)$$

where the function $F(a)$ has limits

$$F(a \rightarrow 0) \rightarrow \frac{1}{2}a^2 - \frac{2}{5}a^4 \quad (70)$$

and

$$F(a \rightarrow \infty) \rightarrow \frac{3}{2}a - (3a)^{1/2} \quad (71)$$

where $a = ZZ_0\alpha Am_p R$. For $0 < a < 1$ the Coulomb model gives a good approximation, while at $2 < a < \infty$ the harmonic oscillator approximation is appropriate.

In the case of OHe $a = ZZ_0\alpha Am_p R \leq 1$, which proves its Bohr-atom-like structure, assumed in References [88,199,209–211]. The radius of Bohr orbit in these “atoms” [88,215] is $r_o \sim 1/(Z_0 Z_{He} \alpha m_{He}) \approx 2 \times 10^{-13} \text{ cm}$. However, the size of the He nucleus rotating around O^{--} in this Bohr atom turns out to be on the order of and even a bit larger than the radius r_o of its Bohr orbit,

and the corresponding correction to the binding energy due to non-point-like charge distribution in He is significant.

The Bohr atom-like structure of OHe seems to provide a possibility to use the results of atomic physics for the description of OHe interaction with matter. However, the situation is much more complicated. The OHe atom is similar to hydrogen, in which the electron is hundreds of times heavier than the proton, so that it is a proton shell that surrounds an “electron nucleus”. Nuclei that interact with such “hydrogen” would interact first with the strongly interacting “protonic” shell, and such interaction can hardly be treated in the framework of perturbation theory. Moreover, in the description of OHe interaction, accounting for the finite size of He—which is even larger than the radius of the Bohr orbit—is important. One should consider, therefore, the analysis presented below as only a first step approaching the true nuclear physics of OHe.

The approach of References [207,215] assumes the following picture of OHe interaction with nuclei: OHe is a neutral atom in the ground state, perturbed by the Coulomb and nuclear forces of the approaching nucleus. The sign of OHe polarization changes with the distance: at larger distances, Stark-like effect takes place—nuclear Coulomb force polarizes OHe so that the nucleus is attracted by the induced dipole moment of OHe, while as soon as the perturbation by nuclear force starts to dominate, the nucleus polarizes OHe in the opposite way so that He is situated more closely to the nucleus, resulting in the repulsive effect of the helium shell of OHe. When helium is completely merged with the nucleus, the interaction is reduced to the oscillatory potential of O^{--} with a homogeneously charged merged nucleus with the charge $Z + 2$.

Therefore OHe-nucleus potential can have a qualitative feature, presented in Figure 2: the potential well at large distances (regions III–IV) is changed by a potential wall in region II. The existence of this potential barrier is crucial for all the qualitative features of the OHe scenario: it causes suppression of reactions with the transition of the OHe-nucleus system to levels in the potential well of the region I, provides the dominance of elastic scattering while transitions to levels in the shallow well (regions III–IV) should dominate in reactions of OHe-nucleus capture. The proof of this picture implies accurate and detailed quantum-mechanical treatment, which was started in Reference [231]. With the use of perturbation theory, it was shown that OHe polarization changes sign as the nucleus approaches OHe (as is given in Figure 3), but the perturbation approach was not valid for the description at smaller distances, while the estimates indicated that this change of polarization may not be sufficient for the creation of the potential, given by Figure 2. If the picture of Figure 2 is not proven, one may need more sophisticated models retaining the ideas of the OHe scenario which involve more elements of new physics, as proposed in Reference [232].

On the other hand, O-helium—being an α -particle with screened electric charge—can catalyze nuclear transformations, which can influence primordial light element abundance and cause primordial heavy element formation. It is especially important for the quantitative estimation of the role of OHe in Big Bang Nucleosynthesis and in stellar evolution. These effects need a special detailed and complicated study of OHe nuclear physics, and this work is under way.

The qualitative picture of OHe cosmological evolution is presented below, following References [87,88,90,199,207,209,215,216], and is based on the idea of the dominant role of elastic collisions in OHe interaction with baryonic matter.

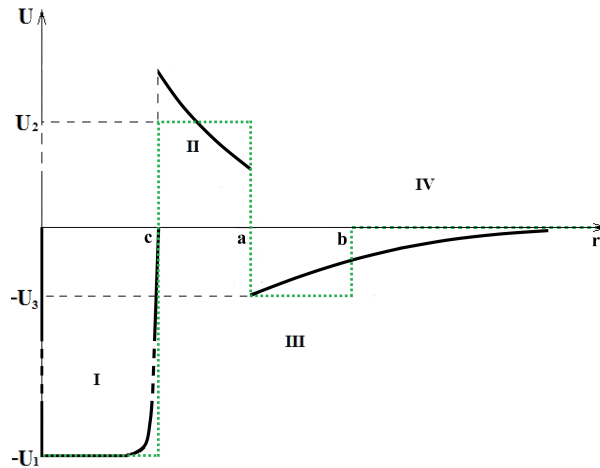


Figure 2. The potential of the O-Helium (OHe)-nucleus system and its rectangular well approximation.

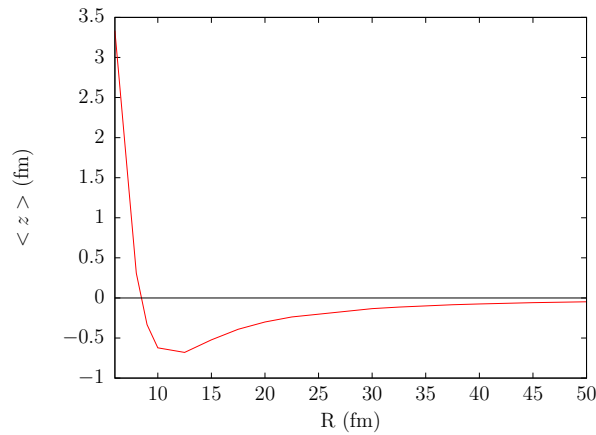


Figure 3. Polarization $\langle z \rangle$ (Fm) of OHe as a function of the distance R (fm) of an external sodium nucleus, calculated in Reference [231] in the framework of perturbation theory. Note that here R denotes the distance between OHe and the nucleus and not radius of the nucleus, as it was in Equations (65), (66), (68), and (69).

5.2. Large Scale Structure Formation by OHe Dark Matter

Due to elastic nuclear interactions of its helium constituent with nuclei in the cosmic plasma, the O-helium gas is in thermal equilibrium with plasma and radiation in the Radiation Dominance (RD) stage, while the energy and momentum transfer from plasma is effective. The radiation pressure acting on the plasma is then transferred to density fluctuations of the O-helium gas, and transforms them in acoustic waves at scales up to the size of the horizon.

At temperature $T < T_{od} \approx 1S_3^{2/3}$ eV, the energy and momentum transfer from baryons to O-helium is not effective [88,199] because

$$n_B \langle \sigma v \rangle (m_p/m_o)t < 1 \tag{72}$$

where m_o is the mass of the OHe atom, and $S_3 = m_o/(1 \text{ TeV})$. Here

$$\sigma \approx \sigma_o \sim \pi r_o^2 \approx 10^{-25} \text{ cm}^2 \tag{73}$$

and $v = \sqrt{2T/m_p}$ is the baryon thermal velocity. Then, O-helium gas decouples from plasma. It starts to dominate in the universe after $t \sim 10^{12}$ s at $T \leq T_{RM} \approx 1$ eV, and O-helium “atoms” play the main dynamical role in the development of gravitational instability, triggering large scale structure

formation. The composite nature of O-helium determines the specifics of the corresponding dark matter scenario.

At $T > T_{RM}$, the total mass of the *OHe* gas with density $\rho_d = (T_{RM}/T)\rho_{tot}$ is equal to

$$M = \frac{4\pi}{3}\rho_d t^3 = \frac{4\pi}{3}\frac{T_{RM}}{T}m_{Pl}\left(\frac{m_{Pl}}{T}\right)^2 \quad (74)$$

within the cosmological horizon $l_h = t$. In the period of decoupling $T = T_{od}$, this mass depends strongly on the O-helium mass S_3 , and is given by [199]

$$M_{od} = \frac{T_{RM}}{T_{od}}m_{Pl}\left(\frac{m_{Pl}}{T_{od}}\right)^2 \approx 2 \times 10^{44}S_3^{-2} \text{ g} = 10^{11}S_3^{-2}M_\odot \quad (75)$$

where M_\odot is the solar mass. O-helium is formed only at T_o and its total mass within the cosmological horizon in the period of its creation is $M_o = M_{od}(T_{od}/T_o)^3 = 10^{37} \text{ g}$.

In the RD stage before decoupling, the Jeans length λ_J of the *OHe* gas was restricted from below by the propagation of sound waves in plasma with a relativistic equation of state $p = \epsilon/3$, being on the order of the cosmological horizon and equal to $\lambda_J = l_h/\sqrt{3} = t/\sqrt{3}$. After decoupling at $T = T_{od}$, it falls down to $\lambda_J \sim v_o t$, where $v_o = \sqrt{2T_{od}/m_o}$. Though, after decoupling, the Jeans mass in the *OHe* gas correspondingly falls down

$$M_J \sim v_o^3 M_{od} \sim 3 \times 10^{-14} M_{od} \quad (76)$$

one should expect a strong suppression of fluctuations on scales $M < M_o$, as well as adiabatic damping of sound waves in the RD plasma for scales $M_o < M < M_{od}$. It can provide some suppression of small scale structure in the considered model for all reasonable masses of O-helium. The significance of this suppression and its effect on structure formation needs a special study in detailed numerical simulations. In any case, it cannot be as strong as the free streaming suppression in ordinary Warm Dark Matter (WDM) scenarios, but one can expect that, qualitatively, we deal with the Warmer Than Cold Dark Matter model.

At temperature $T < T_{od} \approx 1S_3^{2/3} \text{ keV}$, the energy and momentum transfer from baryons to O-helium is not effective [88,207,215], and O-helium gas decouples from plasma. It starts to dominate in the universe after $t \sim 10^{12} \text{ s}$ at $T \leq T_{RM} \approx 1 \text{ eV}$, and O-helium “atoms” play the main dynamical role in the development of gravitational instability, triggering large scale structure formation. The composite nature of O-helium determines the specifics of the corresponding warmer than cold dark matter scenario.

Being decoupled from baryonic matter, the *OHe* gas does not follow the formation of baryonic astrophysical objects (stars, planets, molecular clouds, etc.) and forms dark matter halos of galaxies. It can be easily seen that O-helium gas is collisionless for its number density, saturating galactic dark matter. Taking the average density of baryonic matter, one can also find that the galaxy as a whole is transparent for O-helium in spite of its nuclear interaction. Only individual baryonic objects like stars and planets are opaque for it.

5.3. Anomalous Component of Cosmic Rays

O-helium atoms can be destroyed in astrophysical processes, giving rise to the acceleration of free O^{--} in the galaxy.

O-helium can be ionized due to nuclear interaction with cosmic rays [88,211]. Estimations [88,233] show that for the number density of cosmic rays $n_{CR} = 10^{-9} \text{ cm}^{-3}$ during the age of a galaxy, a fraction of about 10^{-6} of the total amount of OHe is disrupted irreversibly, since the inverse effect of recombination of free O^{--} is negligible. Near the solar system, it leads to the concentration of free O^{--} $n_O = 3 \times 10^{-10} S_3^{-1} \text{ cm}^{-3}$. After OHe destruction, free O^{--} have momentum of order $p_O \cong \sqrt{2 \cdot m_o \cdot I_o} \cong 2 \text{ GeV}S_3^{1/2}$ and velocity $v/c \cong 2 \times 10^{-3} S_3^{-1/2}$, and due to effect of Solar

modulation these particles initially can hardly reach Earth [208,233]. Their acceleration by Fermi mechanism or by collective acceleration forms the power spectrum of the O^{--} component at the level of $O/p \sim n_O/n_g = 3 \times 10^{-10} S_3^{-1}$, where $n_g \sim 1 \text{ cm}^{-3}$ is the density of baryonic matter gas.

At the stage of red supergiant, stars have the size $\sim 10^{15} \text{ cm}$, and during the period of this stage $\sim 3 \times 10^{15} \text{ s}$, up to $\sim 10^{-9} S_3^{-1}$ of O-helium atoms per nucleon can be captured [208,233]. In the Supernova explosion, these OHe atoms are disrupted in collisions with particles in the front of the shock wave and the acceleration of free O^{--} by the regular mechanism gives the corresponding fraction in cosmic rays. However, this picture needs detailed analysis, based on the development of OHe nuclear physics and numerical studies of OHe evolution in the stellar matter.

If these mechanisms of O^{--} acceleration are effective, the anomalous low Z/A component of -2 charged O^{--} can be present in cosmic rays at the level $O/p \sim n_O/n_g \sim 10^{-9} S_3^{-1}$, and be within the reach for PAMELA and AMS02 cosmic ray experiments.

In the framework of the Walking Technicolor model, the excess of both stable ζ^{--} and $(UU)^{++}$ is possible [208]; the latter being two to three orders of magnitude smaller than the former. This leads to the two-component composite dark matter scenario, with the dominant OHe accompanied by a subdominant WIMP-like component of $(\zeta^{--}(UU)^{++})$ bound systems. Technibaryons can be metastable, and decays of $(UU)^{++}$ can provide an explanation for anomalies observed in the high energy cosmic positron spectrum by PAMELA, FERMI-LAT, and AMS02.

5.4. Positron Annihilation and Gamma Lines in Galactic Bulge

Inelastic interaction of O-helium with matter in the interstellar space and its de-excitation can give rise to radiation in the range from a few keV to a few MeV. In the galactic bulge with radius $r_b \sim 1 \text{ kpc}$, the number density of O-helium can reach the value $n_o \approx 3 \times 10^{-3} / S_3 \text{ cm}^{-3}$, and the collision rate of O-helium in this central region was estimated in [211]: $dN/dt = n_o^2 \sigma v_h 4\pi r_b^3 / 3 \approx 3 \times 10^{42} S_3^{-2} \text{ s}^{-1}$. At the velocity of $v_h \sim 3 \times 10^7 \text{ cm/s}$, energy transfer in such collisions is $\Delta E \sim 1 \text{ MeV} S_3$. These collisions can lead to the excitation of O-helium. If the 2S level is excited, pair production dominates over two-photon channel in the de-excitation by $E0$ transition, and positron production with the rate $3 \times 10^{42} S_3^{-2} \text{ s}^{-1}$ is not accompanied by strong gamma signal. According to Reference [234], this rate of positron production for $S_3 \sim 1$ is sufficient to explain the excess in positron annihilation line from bulge, measured by INTEGRAL (see Reference [235] for review and references). If OHe levels with nonzero orbital momentum are excited, gamma lines should be observed from transitions $(n > m) E_{nm} = 1.598 \text{ MeV} (1/m^2 - 1/n^2)$ (or from the similar transitions corresponding to the case $I_o = 1.287 \text{ MeV}$) at the level $3 \times 10^{-4} S_3^{-2} (\text{cm}^2 \text{ s MeVster})^{-1}$.

5.5. O-Helium Solution for Dark Matter Puzzles

It should be noted that the nuclear cross section of the O-helium interaction with matter escapes the severe constraints [225–227] on strongly-interacting dark matter particles (SIMPs) [219–227] imposed by the XQC experiment [236,237]. Therefore, a special strategy of direct O-helium search is needed, as proposed in [238].

5.5.1. O-Helium in the Terrestrial Matter

The evident consequence of the O-helium dark matter is its inevitable presence in the terrestrial matter, which appears opaque to O-helium and stores all its in-falling flux.

After they fall down to the terrestrial surface, the in-falling OHe particles are effectively slowed down due to elastic collisions with matter. They then drift, sinking down towards the center of the Earth with velocity

$$V = \frac{g}{n\sigma v} \approx 80 S_3 A_{med}^{1/2} \text{ cm/s} \quad (77)$$

Here $A_{med} \sim 30$ is the average atomic weight in terrestrial surface matter, $n = 2.4 \times 10^{24} / A$ is the number of terrestrial atomic nuclei, σv is the rate of nuclear collisions, and $g = 980 \text{ cm/s}^2$.

Near the Earth's surface, the O-helium abundance is determined by the equilibrium between the in-falling and down-drifting fluxes.

At a depth L below the Earth's surface, the drift timescale is $t_{dr} \sim L/V$, where $V \sim 400 S_3 \text{ cm/s}$ is the drift velocity and $m_o = S_3 \text{ TeV}$ is the mass of O-helium. This means that the change of the incoming flux, caused by the motion of the Earth along its orbit, should lead at the depth $L \sim 10^5 \text{ cm}$ to the corresponding change in the equilibrium underground concentration of OHe on the timescale $t_{dr} \approx 2.5 \times 10^2 S_3^{-1} \text{ s}$.

The equilibrium concentration—which is established in the matter of underground detectors at this timescale—is given by

$$n_{oE} = n_{oE}^{(1)} + n_{oE}^{(2)} \cdot \sin(\omega(t - t_0)) \quad (78)$$

with $\omega = 2\pi/T$, $T = 1yr$ and t_0 the phase. So, there is an averaged concentration given by

$$n_{oE}^{(1)} = \frac{n_o}{320 S_3 A_{med}^{1/2}} V_h \quad (79)$$

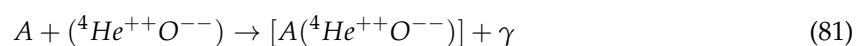
and the annual modulation of concentration characterized by the amplitude

$$n_{oE}^{(2)} = \frac{n_o}{640 S_3 A_{med}^{1/2}} V_E \quad (80)$$

Here V_h is the speed of Solar System (220 km/s), V_E is the speed of the Earth (29.5 km/s), and $n_o = 3 \times 10^{-4} S_3^{-1} \text{ cm}^{-3}$ is the local density of O-helium dark matter.

5.5.2. OHe in the Underground Detectors

The explanation [90,215,218] of the results of the DAMA/NaI [69] and DAMA/LIBRA [70] (see Reference [71] for the latest review of these results) experiments is based on the idea that OHe—slowed down in the matter of detector—can form a few keV bound state with a nucleus, in which OHe is situated beyond the nucleus. Therefore, the positive result of these experiments is explained by annual modulation in reaction of radiative capture of OHe



by nuclei in DAMA detector.

To simplify the solution of the Schrödinger equation, the potential was approximated in References [207,215] by a rectangular potential, presented in Figure 2. The solution of the Schrödinger equation determines the condition under which a low-energy OHe-nucleus bound state appears in the shallow well of region III and the range of nuclear parameters was found at which OHe-sodium binding energy is in the interval 2–4 keV.

The rate of radiative capture of OHe by nuclei can be calculated [215,218] with the use of the analogy with the radiative capture of a neutron by a proton, accounting for: (i) absence of M1 transition that follows from the conservation of orbital momentum; and (ii) suppression of E1 transition in the case of OHe. Since OHe is isoscalar, the isovector E1 transition can take place in the OHe-nucleus system only due to the effect of isospin nonconservation, which can be measured by the factor $f = (m_n - m_p)/m_N \approx 1.4 \times 10^{-3}$, corresponding to the difference of mass of neutron, m_n , and proton, m_p , relative to the mass of nucleon, m_N . In the result, the rate of OHe radiative capture by a nucleus with atomic number A and charge Z to the energy level E in a medium with temperature T is given by

$$\sigma v = \frac{f\pi\alpha}{m_p^2} \frac{3}{\sqrt{2}} \left(\frac{Z}{A}\right)^2 \frac{T}{\sqrt{Am_p E}} \quad (82)$$

Formation of an OHe-nucleus bound system leads to energy release of its binding energy, detected as ionization signal. In the context of our approach, the existence of annual modulations of this signal

in the range 2–6 keV and the absence of such an effect at energies above 6 keV means that binding energy E_{Na} of the Na-OHe system in the DAMA experiment should not exceed 6 keV, being in the range 2–4 keV. The amplitude of annual modulation of the ionization signal can reproduce the result of DAMA/NaI and DAMA/LIBRA experiments for $E_{Na} = 3$ keV. Accounting for the energy resolution in DAMA experiments [239] can explain the observed energy distribution of the signal from a monochromatic photon (with $E_{Na} = 3$ keV) emitted in OHe radiative capture.

At the corresponding nuclear parameters, there is no binding of OHe with iodine and thallium [215].

It should be noted that the results of the DAMA experiment also exhibit the absence of annual modulations of the energy above 1 MeV. Energy release in this range should take place if the OHe-nucleus system comes to the deep level inside the nucleus. This transition implies tunneling through dipole Coulomb barrier, and is suppressed below the experimental limits.

For the chosen range of nuclear parameters, reproducing the results of DAMA/NaI and DAMA/LIBRA, the results of Reference [215,240] indicate that there are no levels in the OHe-nucleus systems for heavy nuclei. In particular, there are no such levels in Xe, which seems to prevent direct comparison with DAMA results in the XENON100 experiment [75]. The existence of such levels in Ge and the comparison with the results of CDMS [72–74] and CoGeNT [76] experiments need special study. According to Reference [215], OHe should bind with O and Ca, which is of interest for interpretation of the signal observed in the CRESST-II experiment [241].

In thermal equilibrium, OHe capture rate is proportional to the temperature. Therefore, it looks like it is suppressed in cryogenic detectors by a factor on the order of 10^{-4} . However, for the size of cryogenic devices (less than a few tens of meters), OHe gas in them has the thermal velocity of the surrounding matter, and this velocity dominates in the relative velocity of the OHe-nucleus system. This gives the suppression relative to room temperature only $\sim m_A/m_o$. Then, the rate of OHe radiative capture in cryogenic detectors is given by Equation (82), in which room temperature T is multiplied by factor m_A/m_o . Note that in the case of $T = 70$ K in the CoGeNT experiment, relative velocity is determined by the thermal velocity of germanium nuclei, which leads to enhancement relative to cryogenic germanium detectors.

5.6. Discussion

The existence of heavy stable particles is one of the popular solutions for the dark matter problem. Usually they are considered to be electrically neutral. However, dark matter can potentially be formed by stable heavy charged particles bound in neutral atom-like states by Coulomb attraction. Analysis of the cosmological data and atomic composition of the universe gives constraints on the particle charge, showing that only -2 charged constituents—being trapped by primordial helium in neutral O-helium states—can avoid the problem of overproduction of the anomalous isotopes of chemical elements, which are severely constrained by observations. A cosmological model of O-helium dark matter can even explain puzzles of direct dark matter searches.

The proposed explanation is based on the mechanism of low-energy binding of OHe with nuclei. Within the uncertainty of nuclear physics parameters, there exists a range at which OHe binding energy with sodium is in the interval 2–4 keV. Annual modulation in radiative capture of OHe to this bound state leads to the corresponding energy release observed as an ionization signal in DAMA/NaI and DAMA/LIBRA experiments.

Accounting for the of the numerical results to the values of nuclear parameters and for the approximations made in the calculations, the presented results can be considered only as an illustration of the possibility of explaining puzzles of the dark matter search in the framework of the composite dark matter scenario. An interesting feature of this explanation is a conclusion that the ionization signal may be absent in detectors containing light (e.g., ^3He) or heavy (e.g., Xe) elements. Therefore, tests of results of the DAMA/NaI and DAMA/LIBRA experiments by other experimental groups can become a very nontrivial task. Recent indications of a positive result in the matter of the CRESST detector [241], in which OHe binding is expected together with absence of signal in xenon detector [75],

may qualitatively favor the presented approach. For the same chemical content, an order of magnitude suppression in cryogenic detectors can explain why a possible positive effect in the CoGeNT experiment [76] can be compatible with the constraints of the CDMS experiment.

The present explanation contains distinct features, by which it can be distinguished from other recent approaches to this problem (see [25] for review and references).

An inevitable consequence of the proposed explanation is the appearance of anomalous superheavy isotopes in the matter of underground detectors, having mass roughly m_0 larger than ordinary isotopes of the corresponding elements.

It is interesting to note that in the framework of the presented approach, positive results of the experimental search for WIMPs by effect of their nuclear recoil would be a signature for a multicomponent nature of dark matter. Such OHe+WIMPs multicomponent dark matter scenarios naturally follow from the AC model [87] and can be realized in models of Walking technicolor [208].

Stable -2 charge states (O^{--}) can be elementary, like AC-leptons or technileptons, or look like technibaryons. The latter, composed of techniquarks, reveal their structure at much higher energy scale and should be produced at the LHC as elementary species. The signature for AC leptons and techniparticles is unique and distinctive, which allows their separation from other hypothetical exotic particles.

Since simultaneous production of three $U\bar{U}$ pairs and their conversion in two doubly charged quark clusters UUU is suppressed, the only possibility to test the models of composite dark matter from fourth generation in the collider experiments is a search for the production of stable hadrons containing single U or \bar{U} -like Uud and $\bar{U}u/\bar{U}d$.

The presented approach sheds new light on the physical nature of dark matter. Specific properties of dark atoms and their constituents are challenging for the experimental search. The development of the quantitative description of OHe interaction with matter confronted with the experimental data will provide the complete test of the composite dark matter model. It challenges the search for stable doubly charged particles at accelerators and cosmic rays as direct experimental probe for charged constituents of the dark atoms of dark matter.

6. Conclusions

The mystical Ouroboros (self-eating-snake) illustrates the main problem of modern fundamental physics: *The theory of the universe is based on the predictions of particle theory, which in turn need cosmology for their test.* Indeed, our modern understanding of the structure and evolution of the universe involves phenomena of inflation, baryosynthesis, and dark matter and dark energy. Cosmoparticle physics [1–3,242,243] offers the way out of this wrong circle. It studies the fundamental basis and mutual relationship between micro-and macro-worlds in the proper combination of physical, astrophysical, and cosmological signatures. Some aspects of this relationship, which arise in the extension of nuclear symmetry to physics beyond the standard model, is the subject of this review.

Acknowledgments: I express my gratitude to Dinesh Shetty for the kind invitation to contribute to this Special issue and to all my co-authors of the original papers, on which the present review is based. I am grateful to J.R. Cudell for reading the manuscript and valuable comments. The work was performed within the framework of the Center FRPP supported by MEPHI Academic Excellence Project (contract 02.03.21.0005, 27.08.2013). The part on initial cosmological conditions was supported by the Ministry of Education and Science of Russian Federation, project 3.472.2014/K and on the forms of dark matter by grant RFBR 14-22-03048.

Conflicts of Interest: The author declares no conflict of interest.

References

1. Khlopov, M.Y. *Cosmoparticle Physics*; World Scientific: Singapore, 1999.
2. Khlopov, M.Y. *Fundamentals of Cosmoparticle Physics*; CISP-Springer: Cambridge, UK, 2012.
3. Khlopov, M.Y. *Cosmoparticle physics: Cross-disciplinary study of physics beyond the standard model. Bled Workshops Phys.* **2006**, *7*, 51–62.

4. Khlopov, M.Y. Direct and indirect astrophysical effects of hypothetical particles and fields. In *Cosmion-94*; Editions Frontieres: Moscow, Russia, 1996.
5. Khlopov, M.Y.; Mankoc-Borstnik, N.S. Proceedings to the 10th workshop 'what comes beyond the standard models. *Bled Workshops Phys.* **2007**, *8*, 114–131.
6. Bertone, G. *Particle Dark Matter: Observations, Models and Searches*; Cambridge University Press: Cambridge, UK, 2010.
7. Frenk, C.S.; White, S.D.M. Dark matter and cosmic structure. *Ann. Phys.* **2012**, *524*, 507–534.
8. Gelmini, G.B. Search for dark matter. *Int. J. Mod. Phys. A* **2008**, *23*, 4273–4288.
9. Aprile, E.; Profumo, S. Focus on dark matter and particle physics. *New J. Phys.* **2009**, *11*, 105002.
10. Feng, J.L. Dark matter candidates from particle physics and methods of detection. *Ann. Rev. Astron. Astrophys.* **2010**, *48*, 495–545.
11. Weinberg, S. *Gravitation and Cosmology*; John Wiley and Sons, Inc.: New York, NY, USA, 1972.
12. Zeldovich, Y.B.; Novikov, I.D. *Structure and Evolution of the Universe*; Nauka: Moscow, Russia, 1985.
13. Starobinsky, A. A new type of isotropic cosmological models without singularity. *Phys. Lett.* **1980**, *91B*, 99–102.
14. Guth, A.H. The inflationary universe: A possible solution to the horizon and flatness problems. *Phys. Rev. D* **1981**, *23*, 347–356.
15. Linde, A.D. A new inflationary universe scenario: A possible solution of the horizon, flatness, homogeneity, isotropy and primordial monopole problems. *Phys. Lett. B* **1982**, *108*, 389–393.
16. Albrecht, A.; Steinhardt, P.J. Cosmology for grand unified theories with radiatively induced symmetry breaking. *Phys. Rev. Lett.* **1982**, *48*, 1220–1223.
17. Linde, A.D. Chaotic inflation. *Phys. Lett. B* **1983**, *129*, 177–181.
18. Sakharov, A.D. Violation of CP invariance, c asymmetry, and baryon asymmetry of the universe. *JETP Lett.* **1967**, *5*, 24–27.
19. Kuzmin, V.A. CP-noninvariance and baryon asymmetry of the universe. *JETP Lett.* **1970**, *12*, 228–230.
20. Linde, A.D. *Particle Physics and Inflationary Cosmology*; Harwood: Chur, Switzerland, 1990.
21. Kolb, E.W.; Turner, M.S. *The Early Universe*; Addison-Wesley: Boston, MA, USA, 1990.
22. Gorbunov, D.S.; Rubakov, V.A. *Introduction to the Theory of the Early Universe Hot Big Bang Theory*; World Scientific: Singapore, 2011.
23. Gorbunov, D.S.; Rubakov, V.A. *Introduction to the Theory of the Early Universe. Cosmological Perturbations and Inflationary Theory*; World Scientific: Singapore, 2011.
24. Carrasco, J.J.M.; Kallosh, R.; Linde, A. Minimal supergravity inflation. *Phys. Rev. D* **2016**, *93*, 061301.
25. Khlopov, M.Y. Fundamental particle structure in the cosmological dark matter. *Int. J. Mod. Phys. A* **2013**, *28*, 1330042.
26. 'tHooft, G. Magnetic monopoles in unified gauge theories. *Nucl. Phys. B* **1974**, *79*, 276–284.
27. Polyakov, A.M. Particle spectrum in quantum field theory. *JETP Lett.* **1974**, *20*, 194–195.
28. Zeldovich, Y.B.; Khlopov, M.Y. On the concentration of relic magnetic monopoles in the universe. *Phys. Lett.* **1978**, *B79*, 239–242.
29. Khlopov, M.Y. Primordial magnetic monopoles. *Priroda* **1979**, *12*, 99–101.
30. Preskill, J.P. Cosmological production of superheavy magnetic monopoles. *Phys. Rev. Lett.* **1979**, *43*, 1365–1374.
31. Khlopov, M.Y. On the concentration of magnetic monopoles in the universe. In *Magnetic Stars*; Nauka: Leningrad, Russia, 1988; p. 201.
32. Zeldovich, Y.B. Cosmological fluctuations produced near a singularity. *Mon. Not. Roy. Astr. Soc.* **1980**, *192*, 663–667.
33. Vilenkin, A. Cosmological density fluctuations produced by vacuum strings. *Phys. Rev. Lett.* **1981**, *46*, 1169–1172.
34. Zeldovich, Y.B.; Kobzarev, I.Y.; Okun, L.B. Cosmological consequences of the spontaneous breakdown of discrete symmetry. *Sov. Phys. JETP* **1975**, *40*, 1–5.
35. Khlopov, M.Y. Primordial black holes. *Res. Astron. Astrophys.* **2010**, *10*, 495–528.
36. Berezhiani, Z.; Khlopov, M.Y. Theory of broken gauge symmetry of families. *Sov. J. Nucl. Phys.* **1990**, *51*, 739–746.

37. Berezhiani, Z.; Khlopov, M.Y. Physical and astrophysical consequences of breaking of the symmetry of families. *Sov. J. Nucl. Phys.* **1990**, *51*, 935–942.
38. Berezhiani, Z.; Khlopov, M.Y.; Khomeriki, R.R. On the possible test of quantum flavor dynamics in the searches for rare decays of heavy particles. *Sov. J. Nucl. Phys.* **1990**, *52*, 344–347.
39. Sakharov, A.S.; Khlopov, M.Y. Horizontal unification as the phenomenology of the theory of “everything”. *Phys. Atom. Nucl.* **1994**, *57*, 651–658.
40. Jungman, G.; Kamionkowski, M.; Griest, K. Supersymmetric dark matter. *Phys. Rept.* **1996**, *267*, 195–373, doi:10.1016/0370-1573(95)00058-5.
41. Zeldovich, Y.B.; Klypin, A.A.; Khlopov, M.Y.; Chechetkin, V.M. Astrophysical bounds on the mass of heavy stable neutral leptons. *Sov. J. Nucl. Phys.* **1980**, *31*, 664–669.
42. Fargion, D.; Khlopov, M.Y.; Konoplich, R.V.; Mignani, R. Bounds on very heavy relic neutrinos by their annihilation in galactic halo. *Phys. Rev. D* **1995**, *52*, 1828–1836, doi:10.1103/PhysRevD.52.1828.
43. Merle, A. keV neutrino model building. *Int. J. Mod. Phys. D* **2013**, *22*, 1330020, doi:10.1142/S0218271813300206.
44. Khlopov, M.Y.; Linde, A.D. Is it easy to save gravitino? *Phys. Lett. B* **1984**, *138*, 265–268.
45. Balestra, F. Annihilation of antiprotons with Helium-4 at low energies and its relationship with the problems of the modern cosmology and models of grand unification. *Sov. J. Nucl. Phys.* **1984**, *39*, 626–631.
46. Levitan, Y.L.; Sobol, I.M.; Khlopov, M.Y.; Chechetkin, V.M. Production of light elements in cascades from energetic antiprotons in early Universe and problems of nuclear cosmoarcheology. *Sov. J. Nucl. Phys.* **1988**, *47*, 109–115.
47. Khlopov, M.Y.; Levitan, Y.L.; Sedel’Nikov, E.V.; Sobol’, I.M. Nonequilibrium cosmological nucleosynthesis of light elements: Calculations by the Monte Carlo method. *Phys. Atom. Nucl.* **1994**, *57*, 1393–1397.
48. Sedel’nikov, E.V.; Filippov, S.S.; Khlopov, M.Y. Kinetic theory of nonequilibrium cosmological nucleosynthesis. *Phys. Atom. Nucl.* **1995**, *58*, 235–242.
49. Jedamzik, K. Did something decay, evaporate, or annihilate during Big Bang nucleosynthesis? *Phys. Rev. D* **2004**, *70*, 063524, doi:10.1103/PhysRevD.70.063524.
50. Kawasaki, M.; Kohri, K.; Moroi, T. Hadronic decay of late-decaying particles and Big-Bang nucleosynthesis. *Phys. Lett.* **2005**, *B625*, 7–12, doi:10.1016/j.physletb.2005.08.045.
51. Lee, T.D.; Yang, C.N. Question of parity conservation in weak interactions. *Phys. Rev.* **1956**, *104*, 254–258, doi:10.1103/PhysRev.104.254.
52. Kobzarev, I.Y.; Okun, L.B.; Pomeranchuk, I.Y. On the possibility of experimental observation of mirror particles. *Sov. J. Nucl. Phys.* **1966**, *3*, 837–841.
53. Zeldovich, Y.B.; Khlopov, M.Y. The neutrino mass in elementary particle physics and in big Bang cosmology. *Sov. Phys. Uspekhi* **1981**, *24*, 755–774, doi:10.1070/PU1981v024n09ABEH004816.
54. Foot, R.; Volkas, R.R. Neutrino physics and the mirror world: How exact parity symmetry explains the solar neutrino deficit, the atmospheric neutrino anomaly and the LSND experiment. *Phys. Rev. D* **1995**, *52*, 6595–6606, doi:10.1103/PhysRevD.52.6595.
55. Blinnikov, S.I.; Khlopov, M.Y. On possible effects of mirror particles. *Sov. J. Nucl. Phys.* **1982**, *36*, 472–474.
56. Blinnikov, S.I.; Khlopov, M.Y. Possible astronomical effects of mirror particles. *Sov. Astron. J.* **1983**, *27*, 371–375.
57. Carlson, E.D.; Glashow, S.L. Nucleosynthesis versus the mirror universe. *Phys. Lett. B* **1987**, *193*, 168–170, doi:10.1016/0370-2693(87)91216-0.
58. Foot, R.; Volkas, R.R. The Exact parity symmetric model and big bang nucleosynthesis. *Astropart. Phys.* **1997**, *7*, 283–295, doi:10.1016/S0927-6505(97)00028-5.
59. Berezhiani, Z.; Comelli, D.; Villante, F. The Early mirror universe: Inflation, baryogenesis, nucleosynthesis and dark matter. *Phys. Lett. B* **2001**, *503*, 362–375, doi:10.1016/S0370-2693(01)00217-9.
60. Berezhiani, Z. Mirror world and its cosmological consequences. *Int. J. Mod. Phys. A* **2004**, *19*, 3775–3806, doi:10.1142/S0217751X04020075.
61. Kolb, E.W.; Seckel, D.; Turner, M.S. The shadow world. *Nature* **1985**, *314*, 415.
62. Khlopov, M.Y. Observational physics of mirror world. *Sov. Astron.* **1991**, *35*, 21–30.
63. Okun, L.B. Mirror particles and mirror matter: 50 years of speculations and search. *Phys. Usp.* **2007**, *50*, 380–389, doi:10.1070/PU2007v050n04ABEH006227.

64. Ciarcelluti, P. Cosmology with mirror dark matter. *Int. J. Mod. Phys. D* **2010**, *19*, 2151–2230, doi:10.1142/S0218271810018438.
65. Sommerfeld, A. Über die beugung und bremsung der elektronen. *Ann. Phys.* **1931**, *11*, 257–330, doi:10.1002/andp.19314030302.
66. Sakharov, A.D. Interaction of an electron and positron in pair production. *Sov.Phys.Usp.* **1991**, *34*, 375–377.
67. Belotsky, K.M.; Khlopov, M.Y.; Shibaev, K.I. Sakharov's enhancement in the effect of 4th generation neutrino. *Gravit. Cosmol. Suppl.* **2000**, *6*, 140–150.
68. Bernabei, R.; Bellia, P.; Cerullia, R.; Montecchia, F.; Amatob, M.; Ignestib, G.; Incicchitti, A.; Prosperib, D.; Daic, C.J.; He, H.L. Search for WIMP annual modulation signature: Results from DAMA/NaI-3 and DAMA/NaI-4 and the global combined analysis. *Phys. Lett. B* **2000**, *480*, 23–31, doi:10.1016/S0370-2693(00)00405-6.
69. Bernabei, R.; Bellia, P.; Cappella, F.; Cerullia, R.; Montecchia, F.; Nozzoli, F.; Incicchitti, A.; Prosperib, D.; Daic, C.J.; Kuang, H.H. Dark matter search. *Riv. Nuovo Cim.* **2003**, *26*, 1–73.
70. Bernabei, R.; Bellia, P.; Cappella, F.; Cerullia, R.; Dai, C.J.; d'Angelo, A.; He, H.L.; Incicchitti, A.; Kuang, H.H.; Ma, J.M. First results from DAMA/LIBRA and the combined results with DAMA/NaI. *Eur. Phys. J. C* **2008**, *56*, 333–355, doi:10.1140/epjc/s10052-008-0662-y.
71. Bernabei, R.; Bellia, P.; d'Angelo, S.; Di Marco, A.; Montecchia, F.; Cappella, F.; d'Angelo, A.; Incicchitti, A.; Caracciolo, V.; Castellano, S. Dark Matter investigation by DAMA at Gran Sasso. *Int. J. Mod. Phys. A* **2013**, *28*, 1330022, doi:10.1142/S0217751X13300226.
72. Abrams, D.; Akerib, D.S., Barnes, P.D., Jr. Exclusion limits on the WIMP nucleon cross-section from the cryogenic dark matter search. *Phys. Rev. D* **2002**, *66*, 122003, doi:10.1103/PhysRevD.66.122003.
73. Akerib, D.S.; Armel-Funkhouser, M.S.; Attisha, M.J.; Young, B.A. Exclusion limits on the WIMP-nucleon cross section from the first run of the cryogenic dark matter search in the soudan underground laboratory. *Phys. Rev. D* **2005**, *72*, 052009, doi:10.1103/PhysRevD.72.052009.
74. Ahmed, Z.; Akerib, D.S.; Arrenberg, S. Search for weakly interacting massive particles with the first five-tower data from the cryogenic dark matter search at the soudan underground laboratory. *Phys. Rev. Lett.* **2009**, *102*, 011301, doi:10.1103/PhysRevLett.102.011301.
75. Aprile, E.; Arisaka, K.; Arneodo, F. First dark matter results from the XENON100 experiment. *Phys. Rev. Lett.* **2010**, *105*, 131302, doi:10.1103/PhysRevLett.105.131302.
76. Aalseth, C.E.; Barbeau, P.S.; Bowden, N.S. Results from a search for light-mass dark matter with a p-type point contact germanium detector. *Phys. Rev. Lett.* **2011**, *106*, 131302, doi:10.1103/PhysRevLett.106.131301.
77. Golubkov, Y.A.; Khlopov, M.Y. Possible effects of the existence of the fourth generation neutrino. *JETP Lett.* **1999**, *69*, 434–440.
78. Fargion, D.; Konoplich, R.V.; Grossi, M.; Khlopov, M.Y. Galactic gamma halo by heavy neutrino annihilations? *Astropart. Phys.* **2000**, *12*, 307–314, doi:10.1016/S0927-6505(99)00094-8.
79. Belotsky, K.M.; Khlopov, M.Y. Astrophysical Signature of the 4th Neutrino. *Gravit. Cosmol. Suppl.* **2002**, *8*, 112–117.
80. Belotsky, K.M.; Fargion, D.; Khlopov, M.Y.; Konoplich, R.V. May heavy neutrinos solve underground and cosmic ray puzzles? *Phys. Atomn. Nucl.* **2008**, *71*, 147–161, doi:10.1007/s11450-008-1016-9.
81. Belotsky, K.M.; Khlopov, M.Y.; Shibaev, K.I. Monochromatic neutrinos from massive fourth generation neutrino annihilation in the Sun and in the Earth. *Part. Nucl. Lett.* **2001**, *108*, 5–17.
82. Belotsky, K.M.; Khlopov, M.Y.; Shibaev, K.I. Monochromatic neutrinos from the annihilation of fourth-generation massive stable neutrino in the Sun and in the Earth. *Phys. Atom. Nucl.* **2002**, *65*, 382–391, doi:10.1134/1.1451957.
83. Belotsky, K.M.; Damour, T.; Khlopov, M.Y. Implications of a solar-system population of massive 4th generation neutrinos for underground searches of monochromatic neutrino-annihilation signals. *Phys. Lett.* **2002**, *B529*, 10–18, doi:10.1016/S0370-2693(02)01234-0.
84. Fargion, D.; Khlopov, M.Y. Tera-leptons shadows over sinister universe. *Gravit. Cosmol.* **2013**, *19*, 219–231, doi:10.1134/S0202289313040063.
85. Belotsky, K.M.; Khlopov, M.Y. Cosmoparticle physics of the 4th generation neutrino. *Gravit. Cosmol.* **2001**, *7*, 189–192.
86. Belotsky, K.M.; Fargion, D.; Khlopov, M.Y.; Konoplich, R.V.; Ryskin, M.G.; Shibaev, K.I. Heavy hadrons of 4th family hidden in our universe and close to detection? *Grav. Cosm. Suppl.* **2005**, *11*, 3–15.

87. Fargion, D.; Khlopov, M.Y.; Stephan, C.A. Cold dark matter by heavy double charged leptons? *Class. Quantum Grav.* **2006**, *23*, 7305–7354.
88. Khlopov, M.Y. Composite dark matter from 4th generation. *JETP Lett.* **2006**, *83*, 1–4.
89. Belotsky, K.M.; Khlopov, M.Y.; Shibaev, K.I. Composite dark matter and its charged constituents. *Gravit. Cosmol.* **2006**, *12*, 1–7.
90. Khlopov, M.Y. Physics of dark matter in the light of dark atoms. *Mod. Phys. Lett. A* **2011**, *26*, 2823–2839, doi:10.1142/S0217732311037194
91. Ibarra, A.; Tran, D.; Weniger, C. Indirect searches for decaying dark matter. *Int. J. Mod. Phys. A* **2013**, *28*, 1330040, doi:10.1142/S0217751X13300408.
92. Adriani, O.; Barbarino, G.C.; Bazilevskaya, G.A.; Bellotti, R.; Boezio, M.; Bogomolov, E.A.; Bonechi, L.; Bonghi, M.; Bonvicini, V.; Bottai, S. An anomalous positron abundance in cosmic rays with energies 1.5–100 GeV. *Nature* **2009**, *458*, 607–609, doi:10.1038/nature07942.
93. Ackermann, M.; Ajello, M.; Allafort, A. Measurement of separate cosmic-ray electron and positron spectra with the Fermi Large Area Telescope. *Phys. Rev. Lett.* **2012**, *108*, 011103, doi:10.1103/PhysRevLett.108.011103.
94. Aguilar, M.; Alberti, G.; Alpat, B. First result from the alpha magnetic spectrometer on the international space station: Precision measurement of the positron fraction in primary cosmic rays of 0.5–350 GeV. *Phys. Rev. Lett.* **2013**, *110*, 141102, doi:10.1103/PhysRevLett.110.141102.
95. Kounine, A. The alpha magnetic spectrometer on the international space station. *Int. J. Mod. Phys. E* **2012**, *21*, 1230005, doi:10.1142/S0218301312300056.
96. Petraki, K.; Volkas, R.R. Review of asymmetric dark matter. *Int. J. Mod. Phys. A* **2013**, *28*, 1330028, doi:10.1142/S0217751X13300287.
97. Glashow, S.L. A Sinister Extension of the Standard Model to $SU(3) \times SU(2) \times SU(2) \times U(1)$, 2005. Available online: <http://arXiv:hep-ph/0504287> (accessed on 29 April 2005).
98. Khlopov, M.Y.; Chechetkin, V.M. Antiprotons in the universe as a cosmological test of grand unification. *Sov. J. Part. Nucl.* **1987**, *18*, 267–288.
99. Doroshkevich, A.G.; Khlopov, M.Y. On the physical nature of dark matter of the Universe. *Sov. J. Nucl. Phys.* **1984**, *39*, 551–553.
100. Doroshkevich, A.G.; Khlopov, M.Y. Formation of structure in the universe with unstable neutrinos. *Mon. Not. R. Astron. Soc.* **1984**, *211*, 279–282.
101. Doroshkevich, A.G.; Klypin, A.A.; Khlopov, M.Y. Cosmological Models with Unstable Neutrinos. *Sov. Astron.* **1988**, *32*, 127–133.
102. Doroshkevich, A.G.; Klypin, A.A.; Khlopov, M.Y. Large-scale structure formation by decaying massive neutrinos. *Mon. Not. R. Astron. Soc.* **1989**, *239*, 923.
103. Berezhiani, Z.G.; Khlopov, M.Y. Physics of cosmological dark matter in the theory of broken family symmetry. *Sov. J. Nucl. Phys.* **1990**, *52*, 60–64.
104. Berezhiani, Z.G.; Khlopov, M.Y. Cosmology of spontaneously broken gauge family symmetry with axion solution of strong CP-problem. *Z. Phys. C Part. Fields* **1991**, *49*, 73–78.
105. Turner, M.S.; Steigman, G.; Krauss, L.M. Flatness of the universe-Reconciling theoretical prejudices with observational data. *Phys. Rev. Lett.* **1984**, *52*, 2090–2093.
106. Gelmini, G.; Schramm, D.N.; Valle, J.W.F. Majorons: A simultaneous solution to the large and small scale dark matter problems. *Phys. Lett. B* **1984**, *146*, 311–317.
107. Sedelnikov, E.V.; Khlopov, M.Y. Cosmic rays as an additional source of information about nonequilibrium processes in the Universe. *Phys. Atom. Nucl.* **1996**, *59*, 1000–1004.
108. Dimopoulos, S.; Esmailzadeh, R.; Starkman, G.D.; Hall, L.J. Is the universe closed by baryons? Nucleosynthesis with a late decaying massive particle. *Astrophys. J.* **1988**, *330*, 545–568, doi:10.1086/166493.
109. Doroshkevich, A.G.; Khlopov, M.Y. Fluctuations of the cosmic background temperature in unstable-particle Cosmologies. *Sov. Astron. Lett* **1985**, *11*, 236–238.
110. Polnarev, A.G.; Khlopov, M.Y. Cosmology, primordial black Holes, and supermassive particles. *Sov. Phys. Uspekhi* **1985**, *28*, 213–232, doi:10.1070/PU1985v028n03ABEH003858.
111. Khlopov, M.Y.; Polnarev, A.G. Primordial black holes as a cosmological test of grand unification. *Phys. Lett. B* **1980**, *97*, 383–387, doi:10.1016/0370-2693(80)90624-3.
112. Polnarev, A.G.; Khlopov, M.Y. Primordial black holes and the ERA of superheavy particle dominance in the early universe. *Sov. Astron.* **1981**, *25*, 406–411.

113. Konoplich, R.V.; Rubin, S.G.; Sakharov, A.S.; Khlopov, M.Yu. Formation of black holes in the first order phase transitions as cosmological test of mechanisms of symmetry breaking. *Phys. Atom. Nucl.* **1999**, *62*, 1593–1600.
114. Khlopov, M.Y.; Rubin, S.G. *Cosmological Pattern of Microphysics in Inflationary Universe*; Springer Science Business Media: Kluwer, Dordrecht, The Netherlands, 2004.
115. Sakharov, A.S.; Khlopov, M.Y. The nonhomogeneity problem for the primordial axion field. *Phys. Atom. Nucl.* **1994**, *57*, 485–487.
116. Sakharov, A.S.; Khlopov, M.Y.; Sokoloff, D.D. Large scale modulation of the distribution of coherent oscillations of a primordial axion field in the Universe. *Phys. Atom. Nucl.* **1996**, *59*, 1005–1010.
117. Sakharov, A.S.; Khlopov, M.Y.; Sokoloff, D.D. The nonlinear modulation of the density distribution in standard axionic CDM and its cosmological impact. *Nucl. Phys. B Proc. Suppl.* **1999**, *72*, 105–109.
118. Jaeckel, J.; Ringwald, A. The low-energy frontier of particle physics. *Ann. Rev. Nucl. Part. Sci.* **2010**, *60*, 405–437, doi:10.1146/annurev.nucl.012809.104433.
119. Kim, J.E. Light pseudoscalars, particle physics and cosmology. *Phys. Rept.* **1987**, *150*, 1–177, doi:10.1016/0370-1573(87)90017-2.
120. Vilenkin, A.; Shellard, E.P.S. *Cosmic Strings and Other Topological Defects*; Cambridge University Press: Cambridge, UK, 1994.
121. Rubin, S.G.; Khlopov, M.Y.; Sakharov, A.S. Primordial black holes from non-equilibrium second order phase transitions. *Gravit. Cosmol. Suppl.* **2000**, *6*, 51–58.
122. Khlopov, M.Y.; Rubin, S.G.; Sakharov, A.S. Strong primordial nonhomogeneities and galaxy formation. *Gravit. Cosmol. Suppl.* **2002**, *8*, 57–65.
123. Rubin, S.G.; Sakharov, A.S.; Khlopov, M.Y. Formation of primordial galactic nuclei at phase transitions in the early Universe. *JETP* **2001**, *92*, 921–929.
124. Dokuchaev, V.; Eroshenko, Y.; Rubin, S. Quasars formation around clusters of primordial black holes. *Grav. Cosmol.* **2005**, *11*, 99–104.
125. Khlopov, M.Y.; Rubin, S.G.; Sakharov, A.S. Primordial structure of massive black hole clusters. *Astropart. Phys.* **2005**, *23*, 265–277, doi:10.1016/j.astropartphys.2004.12.002.
126. Chechetkin, V.M.; Khlopov, M.Y.; Sapozhnikov, M.G.; Zeldovich, Y.B. Astrophysical aspects of antiproton interaction with He (Antimatter in the Universe). *Phys. Lett. B* **1982**, *118*, 329–332, doi:10.1016/0370-2693(82)90196-4.
127. Dolgov, A.D. Matter and antimatter in the universe. *Nucl. Phys. Proc. Suppl.* **2002**, *113*, 40–49, doi:10.1016/S0920-5632(02)01821-2.
128. Dolgov, A.; Silk, J. Baryon isocurvature fluctuations at small scales and baryonic dark matter. *Phys. Rev. D* **1993**, *47*, 4244–4255.
129. Dolgov, A.D.; Kawasaki, M.; Kevlishvili, N. Inhomogeneous baryogenesis, cosmic antimatter, and dark matter. *Nucl. Phys. B* **2009**, *807*, 229–250, doi:10.1016/j.nuclphysb.2008.08.029.
130. Khlopov, M.Y.; Rubin, S.G.; Sakharov, A.S. Possible origin of antimatter regions in the baryon dominated universe. *Phys. Rev. D* **2000**, *62*, 083505, doi:10.1103/PhysRevD.62.083505.
131. Khlopov, M.Y. An antimatter globular cluster in our galaxy: A probe for the origin of matter. *Gravit. Cosmol.* **1998**, *4*, 69–72.
132. Golubkov, Y.A.; Khlopov, M.Y. Anti-protons annihilation in the galaxy as a source of diffuse gamma background. *Phys. Atom. Nucl.* **2001**, *64*, 1821–1829, doi:10.1134/1.1414930.
133. Belotsky, K.M.; Golubkov, Y.A.; Khlopov, M.Y.; Konoplich, R.V.; Sakharov, A.S. Anti-helium flux as a signature for antimatter globular clusters in our galaxy. *Phys. Atom. Nucl.* **2000**, *63*, 233–239, doi:10.1134/1.855627.
134. Fargion, D.; Khlopov, M.Y. Antimatter bounds by anti-asteroids annihilations on planets and sun. *Astropart. Phys.* **2003**, *19*, 441–446, doi:10.1016/S0927-6505(02)00241-4.
135. Blinnikov, S.I.; Dolgov, A.D.; Postnov, K.A. Antimatter and antistars in the universe and in the Galaxy. *Phys. Rev. D* **2015**, *92*, 023516, doi:10.1103/PhysRevD.92.023516.
136. Khlopov, M.Y. Primordial nonlinear structures and massive black holes from early Universe. *J. Phys. Conf. Ser.* **2007**, *66*, 012032.
137. Oppenheimer, J.R.; Sneider, H. On continued gravitational contraction. *Phys. Rev.* **1939**, *56*, 455–459.
138. Zeldovich, Y.B.; Novikov, I.D. *Relativistic Astrophysics: Stars and Relativity*; University of Chicago Press: Chicago, IL, USA, 1971; Volume 1.

139. Zeldovich, Y.B.; Novikov, I.D. The hypothesis of cores retarded during expansion and the hot cosmological model. *Sov. Astron.* **1967**, *10*, 602–609.
140. Hawking, S.W. Gravitationally collapsed objects of very low mass. *Mon. Not. R. Astron. Soc.* **1971**, *152*, 75–78.
141. Carr, B.J.; Hawking, S.W. Black holes in the early Universe. *Mon. Not. R. Astron. Soc.* **1974**, *168*, 399–415.
142. Bullock, J.S.; Primack, J.R. NonGaussian fluctuations and primordial black holes from inflation. *Phys. Rev. D* **1997**, *55*, 7423–7439.
143. Carr, B.J. The primordial black hole mass spectrum. *Astroph. J.* **1975**, *201*, 1–19, doi:10.1086/153853.
144. Polnarev, A.G.; Khlopov, M.Y. Dustlike stages in the early universe and constraints on the primordial black-hole spectrum. *Sov. Astron.* **1982**, *26*, 391–395.
145. Khlopov, M.Y.; Polnarev, A.G. Superheavy particles in cosmology and evolution of inhomogeneities in the early Universe. In *The Very Early Universe*; Gibbons, G., Hawking, S., Siclos, E., Eds.; Cambridge University Press: Cambridge, UK, 1983; pp. 407–432.
146. Khlopov, M.Y.; Malomed, B.A.; Zel'dovich, Y.B. Gravitational instability of scalar fields and formation of primordial black holes. *Mon. Not. R. Astron. Soc.* **1985**, *215*, 575–589.
147. Zeldovich, Y.B.; Podurets, M.A. The evolution of a system of gravitationally interacting point masses. *Sov. Astron.* **1965**, *9*, 742–748.
148. Gurzadian, V.G.; Savvidi, G.K. Collective relaxation of stellar systems. *Astrophys. J.* **1986**, *160*, 203–210.
149. Kalashnikov, O.K.; Khlopov, M.Y. On the possibility of checking the cosmology of asymptotically free SU(5) theory. *Phys. Lett.* **1983**, *127B*, 407–422, doi:10.1016/0370-2693(83)90281-2.
150. Kadnikov, A.F.; Maslyankin, V.I.; Khlopov, M.Y. Modelling of evolution of quasi-stellar systems, formed by particles and antiparticles in early Universe. *Astrophysics* **1990**, *31*, 523–531, doi:10.1007/BF01004401.
151. Kofman, L.A.; Linde, A.D. Generation of density perturbations in the inflationary cosmology. *Nucl. Phys. B* **1987**, *282*, 555–626, doi:10.1016/0550-3213(87)90698-5.
152. Sakharov, A.S.; Khlopov, M.Y. Cosmological signatures of family symmetry breaking in multicomponent inflation models. *Phys. Atom. Nucl.* **1993**, *56*, 412–417.
153. Watkins, R.; Widrow, M. Aspects of reheating in first order inflation. *Nucl. Phys. B* **1992**, *374*, 446–468.
154. Hawking, S.W.; Moss, I.G.; Stewart, J.M. Bubble collisions in the very early universe. *Phys. Rev. D* **1982**, *26*, 2681–2693, doi:10.1103/PhysRevD.26.2681.
155. Moss, I.G. Singularity formation from colliding bubbles. *Phys. Rev. D* **1994**, *50*, 676–681, doi:10.1103/PhysRevD.50.676.
156. Konoplich, R.V.; Rubin, S.G.; Sakharov, A.S.; Khlopov, M.Y. Formation of black holes in first-order phase transitions in the Universe. *Astron. Lett.* **1998**, *24*, 413–417.
157. Khlopov, M.Y.; Konoplich, R.V.; Rubin, S.G.; Sakharov, A.S. First-order phase transitions as a source of black holes in the early universe. *Gravit. Cosmol.* **2000**, *6*, 153–156.
158. La, D.; Steinhardt, P.J. Extended inflationary cosmology. *Phys. Rev. Lett.* **1989**, *62*, 376–378, doi:10.1103/PhysRevLett.62.376.
159. Holman, R.; Kolb, E.W.; Wang, Y. Gravitational couplings of the inflaton in extended inflation. *Phys. Rev. Lett.* **1990**, *62*, 17–20, doi:10.1103/PhysRevLett.65.17.
160. Holman, R.; Kolb, E.W.; Vadas, S.L.; Wang, Y. Scale invariant extended inflation. *Phys. Rev. D* **1991**, *43*, 3833–3845, doi:10.1103/PhysRevD.43.3833.
161. Adams, F.C.; Freese, K. Double field inflation. *Phys. Rev. D* **1991**, *43*, 353–361, doi:10.1103/PhysRevD.43.353.
162. Copeland, E.J.; Liddle, A.R.; Lyth, D.H.; Stewart, E.D.; Wands, D. False vacuum inflation with Einstein gravity. *Phys. Rev. D* **1994**, *49*, 6410–6433, doi:10.1103/PhysRevD.49.6410.
163. Occhionero, F.; Amendola, L. Primordial bubbles from quadratic gravity. *Phys. Rev. D* **1994**, *50*, 4846–4852, doi:10.1103/PhysRevD.50.4846.
164. Amendola, L.; Baccigalupi, C.; Konoplich, R. Reconstruction of the bubble nucleating potential. *Phys. Rev. D* **1996**, *54*, 7199–7206, doi:10.1103/PhysRevD.54.7199.
165. Turner, M.S.; Weinberg, E.J.; Widrow, L.M. Bubble nucleation in first order inflation and other cosmological phase transitions. *Phys. Rev. D* **1992**, *46*, 2384–2403, doi:10.1103/PhysRevD.46.2384.
166. Hawking, S.W. Particle creation by black holes. *Comm. Math. Phys.* **1975**, *43*, 199–220, doi:10.1007/BF02345020.
167. Hawking, S.W. Black hole explosions. *Nature* **1974**, *248*, 30–31, doi:10.1038/248030a0.
168. Carr, B.J.; Gilbert, J.H.; Lidsey, J.E. Black hole relics and inflation: Limits on blue perturbation spectra. *Phys. Rev. D* **1994**, *50*, 4853–4867, doi:10.1103/PhysRevD.50.4853.

169. Barrow, J.D.; Copeland, E.J.; Liddle, A.R. The cosmology of black hole relics. *Phys. Rev. D* **1992**, *46*, 645–657, doi:10.1103/PhysRevD.46.645.
170. Alexeyev, S.O.; Pomazanov, M.V. Black hole solutions with dilatonic hair in higher curvature gravity. *Phys. Rev. D* **1997**, *55*, 2110–2118, doi:10.1103/PhysRevD.55.2110.
171. Dymnikova, I.G. De sitter-schwarzschild black hole: Its particlelike core and thermodynamical properties. *Int. Jour. Mod. Phys. D* **1996**, *5*, 529–540, doi:10.1142/S0218271896000333.
172. Miyama, S.; Sato, K. The upper bound of the number density of primordial black holes from the big bang nucleosynthesis. *Prog. Theor. Phys.* **1978**, *59*, 1012–1013, doi:10.1143/PTP.59.1012.
173. Zeldovich, Y.B.; Starobinsky, A.A. Possibility of a cold cosmological singularity in the spectrum of primordial black holes. *JETP Lett.* **1976**, *24*, 571–573.
174. Naselsky, P.D. Hydrogen recombination kinetics in the presence of low-mass primordial black holes. *Sov. Astron. Lett.* **1978**, *4*, 209–211.
175. Lindley, D. Primordial black holes and the deuterium abundance. *Mon. Not. R. Astron. Soc.* **1980**, *193*, 593–601, doi:10.1093/mnras/193.3.593.
176. Zeldovich, Y.B.; Starobinskii, A.A.; Khlopov, M.I.; Chechetkin, V.M. Primordial black holes and the deuterium problem. *Sov. Astron. Lett.* **1977**, *3*, 110–112.
177. Rothman, T.; Matzner, R. Upper limits on micro-mini black holes. *Astrophys. Space. Sci.* **1981**, *75*, 229–236, doi:10.1007/BF00648639.
178. MacGibbon, J.H.; Carr, B.J. Cosmic rays from primordial black holes. *Astrophys. J.* **1991**, *371*, 447–469, doi:10.1086/169909.
179. Novikov, I.D.; Polnarev, A.G.; Starobinskii, A.A.; Zeldovich, I.B. Primordial black holes. *Astron. Astrophys.* **1979**, *80*, 104–109.
180. Chechetkin, V.M.; Khlopov, M.Y.; Sapozhnikov, M.G. Antiproton interactions with light elements as a test of GUT cosmology. *Riv. Nuovo Cim.* **1982**, *5*, 1–79, doi:10.1007/BF02740484.
181. MacGibbon, J.H.; Carr, B.J. Cosmic rays from primordial black holes and constraints on the early universe. *Phys. Rept.* **1998**, *307*, 141–154, doi:10.1016/S0370-1573(98)00039-8.
182. Liddle, A.R.; Green, A.M. Cosmological constraints from primordial black holes. *Phys. Rept.* **1998**, *307*, 125–131, doi:10.1016/S0370-1573(98)00069-6.
183. Lemoine, M. Moduli constraints on primordial black holes. *Phys. Lett. B* **2000**, *481*, 333–338, doi:10.1016/S0370-2693(00)00469-X.
184. Green, A.M. Supersymmetry and primordial black hole abundance constraints. *Phys. Rev. D* **1998**, *60*, 063516, doi:10.1103/PhysRevD.60.063516.
185. Khlopov, M.Y.; Barrau, A.; Grain, J. Gravitino production by primordial black hole evaporation and constraints on the inhomogeneity of the early Universe. *Class. Quantum Grav.* **2006**, *23*, 1875–1882, doi:10.1088/0264-9381/23/6/004.
186. Carr, B.J. Primordial black holes as a probe of cosmology and high energy physics. *Lect. Notes Phys.* **2003**, *631*, 301–321.
187. Blais, D.; Kiefer, C.; Polarski, D. Can primordial black holes be a significant part of dark matter? *Phys. Lett. B* **2002**, *535*, 11–16.
188. Afshordi, N.; McDonald, P.; Spergel, D.N. Primordial black holes as dark matter: The power spectrum and evaporation of early structures. *Astrophys. J.* **2003**, *594*, L71–L74.
189. Appelquist, T.; Bai, Y.; Piai, M. SU(3) family gauge symmetry and the axion. *Phys. Rev. D* **2007**, *75*, 073005, doi:10.1103/PhysRevD.75.073005.
190. Appelquist, T.; Bai, Y.; Piai, M. Neutrinos and SU(3) family gauge symmetry. *Phys. Rev. D* **2006**, *74*, 076001, doi:10.1103/PhysRevD.74.076001.
191. Appelquist, T.; Bai, Y.; Piai, M. Quark mass ratios and mixing angles from SU(3) family gauge symmetry. *Phys. Lett. B* **2006**, *637*, 245–250, doi:10.1016/j.physletb.2006.04.043.
192. Chkareuli, J.L. Quark-Lepton families: From SU(5) to SU(8) symmetry. *JETP Lett.* **1980**, *32*, 671–674.
193. Berezhiani, Z.G.; Chkareuli, J.L. Mass of the T quark and the number of quark lepton generations. *JETP Lett.* **1982**, *35*, 612–615.
194. Berezhiani, Z.G.; Chkareuli, J.L. Neutrino oscillations in grand unified models with a horizontal symmetry. *JETP Lett.* **1983**, *37*, 338–341.

195. Berezhiani, Z.G. The weak mixing angles in gauge models with horizontal symmetry: A new approach to quark and lepton masses. *Phys. Lett. B* **1983**, *129*, 99–102. doi:10.1016/0370-2693(83)90737-2.
196. Belotsky, K.M.; Fargion, D.; Khlopov, M.Y. Heavy hadrons of 4th family hidden in our universe and close to detection? *Gravit. Cosmol.* **2005**, *11*, 3–15.
197. Belotsky, K.; Khlopov, M.Y.; Shibaev, K.I. *The Physics of Quarks: New Research*; Watson, N.L., Grant, T.M., Eds.; NOVA Publishers: Hauppauge, NY, USA, 2009; p. 19.
198. Connes, A. *Noncommutative Geometry*; Academic Press: San Diego, CA, USA, 1994.
199. Khlopov, M.Y.; Kouvaris, C. Strong interactive massive particles from a strong coupled theory. *Phys. Rev. D* **2008**, *77*, 065002, doi:10.1103/PhysRevD.77.065002.
200. Sannino, F.; Tuominen, K. Orientifold theory dynamics and symmetry breaking. *Phys. Rev. D* **2005**, *71*, 051901, doi:10.1103/PhysRevD.71.051901.
201. Hong, D.K.; Hsu, S.D.H.; Sannino, F. Composite higgs from higher representations. *Phys. Lett. B* **2004**, *597*, 89–93.
202. Dietrich, D.D.; Sannino, F.; Tuominen, K. Light composite higgs from higher representations versus electroweak precision measurements: Predictions for LHC. *Phys. Rev. D* **2005**, *72*, 055001.
203. Dietrich, D.D.; Sannino, F.; Tuominen, K. Light composite higgs and precision electroweak measurements on the Z resonance: An update. *Phys. Rev. D* **2006**, *73*, 037701.
204. Gudnason, S.B.; Kouvaris, C.; Sannino, F. Towards working technicolor: Effective theories and dark matter. *Phys. Rev. D* **2006**, *73*, 115003.
205. Gudnason, S.B.; Kouvaris, C.; Sannino, F. Dark matter from new technicolor theories. *Phys. Rev. D* **2006**, *74*, 095008.
206. Mankoč Borštnik, N.S. The spin-charge-family theory is explaining the origin of families, of the Higgs and the Yukawa couplings. *Bled Workshops Phys.* **2010**, *11*, 105–129.
207. Khlopov, M.Y.; Mayorov, A.G.; Soldatov, E.Y. Dark atoms of the universe: towards OHe nuclear physics. *Bled Workshops Phys.* **2010**, *11*, 73–88.
208. Khlopov, M.Y.; Kouvaris, C. Composite dark matter from a model with composite Higgs boson. *Phys. Rev. D* **2008**, *78*, 065040.
209. Khlopov, M.Y. The puzzles of dark matter searches. *AIP Conf. Proc.* **2010**, *1241*, 388–397.
210. Khlopov, M.Y.; Mayorov, A.G.; Soldatov, E.Y. Composite dark matter and puzzles of dark matter searches. *Int. J. Mod. Phys. D* **2010**, *19*, 1385–1395.
211. Khlopov, M.Y. Composite Dark Matter from Stable Charged Constituents. Available online: <http://arxiv.org/abs/0806.3581> (accessed on 22 June 2008).
212. Maltoni, M.; Novikov, V.A.; Okun, L.B.; Rozanov, A.N.; Vysotsky, M.I. Extra quark lepton generations and precision measurements. *Phys. Lett. B* **2000**, *476*, 107–115.
213. Khlopov, M.Y.; Shibaev, R.M. Probes for 4th generation constituents of dark atoms in Higgs boson studies at the LHC. *Adv. High Energy Phys.* **2014**, *2014*, 406458, doi:10.1155/2014/406458.
214. Belotsky, K.M.; Fargion, D.; Khlopov, M.Y.; Konoplich, R.V.; Shibaev, K.I. Heavy neutrinos of 4th generation in searches for dark matter. *Gravit. Cosmol.* **2005**, *11*, 16–26.
215. Khlopov, M.Y.; Mayorov, A.G.; Soldatov, E.Y. Puzzles of dark matter in the light of dark atoms. *J. Phys. Conf. Ser.* **2011**, *309*, 012013.
216. Khlopov, M.Y. Dark Matter from Stable Charged Particles? Available online: <http://arxiv.org/abs/0801.0167> (accessed on 30 December 2007).
217. Khlopov, M.Y. Primordial Heavy Elements in Composite Dark Matter Models. Available online: <http://arxiv.org/abs/0801.0169> (accessed on 31 December 2007).
218. Khlopov, M.Y.; Mayorov, A.G.; Soldatov, E.Y. Puzzles of dark matter—more light on dark atoms? *Bled Workshops Phys.* **2010**, *11*, 186–193.
219. Dover, C.B.; Gaiser, T.K.; Steigman, G. Cosmological constraints on new stable hadrons. *Phys. Rev. Lett.* **1979**, *42*, 1117–1120, doi:10.1103/PhysRevLett.42.1117.
220. Wolfram, S. Abundances of stable particles produced in the early universe. *Phys. Lett. B* **1979**, *82*, 65–68, doi:10.1016/0370-2693(79)90426-X.
221. Starkman, G.D.; Gould, A.; Esmailzadeh, R.; Dimopoulos, S. Opening the window on strongly interacting dark matter. *Phys. Rev. D* **1990**, *41*, 3594–3603, doi:10.1103/PhysRevD.41.3594.

222. Javoresek, D.; Elmore, D.; Fischbach, E.; Granger, D.; Miller, T.; Oliver, D.; Teplitz, V. New experimental limits on strongly interacting massive particles at the TeV scale. *Phys. Rev. Lett.* **2001**, *87*, 231804, doi:10.1103/PhysRevLett.87.231804.
223. Mitra, S. Uranus's anomalously low excess heat constrains strongly interacting dark matter. *Phys. Rev. D* **2004**, *70*, 103517, doi:10.1103/PhysRevD.70.103517.
224. Mack, G.D.; Beacom, J.F.; Bertone, G. Towards closing the window on strongly interacting dark matter: Far-reaching constraints from Earth's heat flow. *Phys. Rev. D* **2007**, *76*, 043523, doi:10.1103/PhysRevD.76.043523.
225. Wandelt, B.D.; Dave, R.; Farrar, G.R.; McGuire, P.C.; Spergel, D.N.; Steinhardt, P.J. Self-Interacting Dark Matter. Available online: <http://arXiv:astro-ph/0006344> (accessed on 24 June 2000).
226. McGuire, P.C.; Steinhardt, P.J. Cracking Open the Window for Strongly Interacting Massive Particles as the Halo Dark Matter. Available online: <http://arxiv.org/abs/astro-ph/0105567> (accessed on 31 May 2001).
227. Zaharijas, G.; Farrar, G.R. A window in the dark matter exclusion limits. *Phys. Rev. D* **2005**, *72*, 083502, doi:10.1103/PhysRevD.72.083502.
228. Cahn, R.N.; Glashow, S.L. Chemical signatures for superheavy elementary particles. *Science* **1981**, *213*, 607–611, doi:10.1126/science.213.4508.607.
229. Pospelov, M. Particle physics catalysis of thermal big bang nucleosynthesis. *Phys. Rev. Lett.* **2007**, *98*, 231301, doi:10.1103/PhysRevLett.98.231301.
230. Kohri, K.; Takayama, F. Big bang nucleosynthesis with long-lived charged massive particles. *Phys. Rev. D* **2007**, *76*, 063507, doi:10.1103/PhysRevD.76.063507.
231. Cudell, J.-R.; Khlopov, M.Y.; Wallemacq, Q. The nuclear physics of OHe. *Bled Workshops Phys.* **2012**, *13*, 10–27.
232. Wallemacq, Q. Milli-interacting Dark Matter. *Phys. Rev. D* **2013**, *88*, 063516.
233. Belotsky, K.M.; Mayorov, A.G.; Khlopov, M.Y. Charged particles of dark matter in cosmic rays. In *Scientific Session NRNU MEPhI-2010*; V.4, P.127; World Scientific Publishing Company: Singapore, 2010.
234. Finkbeiner, D.P.; Weiner, N. Exciting dark matter and the INTEGRAL/SPI 511 keV signal. *Phys. Rev. D* **2007**, *76*, 083519, doi:10.1103/PhysRevD.76.083519.
235. Teegarden, B.J.; Watanabe, K.; Jean, P.; Knödlseider, J.; Lonjou, V.; Roques, J.P.; Skinner, G.K.; von Ballmoos, P.; Weidenspointner, G.; Bazzano, A.; et al. INTEGRAL SPI limits on electron-positron annihilation radiation from the galactic plane. *Astrophys. J.* **2005**, *621*, 296–300, doi:10.1086/426859.
236. McCammon, D.; Almy, R.; Deiker, S.; Morgenthaler, J.; Kelley, R.L.; Marshall, F.J.; Moseley, S.H.; Stahle, C.K.; Szymkowiak, A.E. A sounding rocket payload for X-ray astronomy employing high-resolution microcalorimeters. *Nucl. Instrum. Methods A* **1996**, *370*, 266–268.
237. McCammon, D.; Almy, R.; Apodaca, E.; Tiest, W.B.; Cui, W.; Deiker, S.; Galeazzi, M.; Juda, M.; Lesser, A.; Miharaet, T. A high spectral resolution observation of the soft X-ray diffuse background with thermal detectors. *Astrophys. J.* **2002**, *576*, 188–203, doi:10.1086/341727.
238. Belotsky, K.; Bunkov, Y.; Godfrin, H.; Khlopov, M.; Konoplich, R. He-3 Experimentum Crucis for Dark Matter Puzzles. Available online: <http://arXiv:astro-ph/0606350> (accessed on 14 June 2006).
239. Angloher, G.; Bauer, M.; Bavykina, I.; Bento, A.; Bucci, C.; Ciemniak, C.; Deuter, G.; von Feilitzsch, F.; Hauff, D.; Huffet, P. Results from 730 kg days of the CRESST-II Dark Matter search. *Eur. Phys. J. C* **2012**, *72*, doi:10.1140/epjc/s10052-012-1971-8.
240. Khlopov, M.Y.; Mayorov, A.G.; Soldatov, E.Y. Low energy binding of composite dark matter with nuclei as a solution for the puzzles of dark matter searches. *Bled Workshops Phys.* **2009**, *10*, 79–94.
241. Bernabei, R.; Belli, P.; Bussolotti, A.; Cappella, F.; Cerulli, R.; Dai, C.J.; d'Angelo, A.; He, H.L.; Incicchitti, A.; Kuang, H.H.; et al. The DAMA/LIBRA apparatus. *Nucl. Instrum. Methods A* **2008**, *592*, 297–315, doi:10.1016/j.nima.2008.04.082.
242. Sakharov, A.D. Cosmoparticle physics—a multidisciplinary science. *Vestnik AN SSSR* **1989**, *4*, 39–40.
243. Khlopov, M.Y. Fundamental cross-disciplinary studies of microworld and Universe. *Vestnik Russ. Acad. Sci.* **2001**, *71*, 1133–1137.

